



**Air Force Avionics Laboratory  
Air Force Systems Command  
Wright-Patterson Air Force Base, Ohio**

***Scattering from Two-Dimensional Bodies with  
Absorber Sheets***

**VALDIS V. LIEPA  
EUGENE F. KNOTT  
THOMAS B. A. SENIOR**

**May 1974**

**Technical Report AFAL-TR-74-119**

**Distribution limited to U.S. Government Agencies only;**

**Test and Evaluation Data; May 1974**

**Other requests for this document must be referred to AFAL/WRP**

**THE UNIVERSITY OF MICHIGAN**

**COLLEGE OF ENGINEERING**

**DEPARTMENT OF ELECTRICAL AND COMPUTER ENGINEERING**

**Radiation Laboratory**

***Administered through:***

**DIVISION OF RESEARCH DEVELOPMENT AND ADMINISTRATION • ANN ARBOR**

## NOTICE

When Government drawings, specifications, or other data are used for any purpose other than in connection with a definitely related Government procurement operation, the United States Government thereby incurs no responsibility nor any obligation whatsoever; and the fact that the Government may have formulated, furnished, or in any way supplied the said drawings, specifications, or other data, is not to be regarded by implication or otherwise as in any manner licensing the holder or any other person or corporation, or conveying any rights or permission to manufacture, use, or sell any patented invention that may in any way be related thereto.

Copies of this report should not be returned unless return is required by security considerations, contractual obligations, or notice on a specific document.

SCATTERING FROM TWO-DIMENSIONAL BODIES  
WITH ABSORBER SHEETS

Valdis V. Liepa  
Eugene F. Knott  
Thomas B. A. Senior

Distribution limited to U. S. Government Agencies only;  
Test and Evaluation Data; May 1974.  
Other requests for this document must be referred to  
AFAL/WRP.

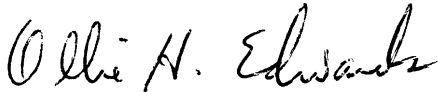
## FOREWORD

This Interim Report describes research performed by The University of Michigan Radiation Laboratory, 2455 Hayward Street, Ann Arbor, Michigan 48105, under USAF Contract F33615-73-C-1174, Project 7633, Task 7633-13, "Non-Specular Radar Cross Section Study." The research was sponsored by the Electromagnetic Division, Air Force Avionics Laboratory, and the Technical Monitor was Dr. Charles H. Kreuger, AFAL/WRP.

The computer program described in the report was developed during the time period 15 October 1973 through 15 March 1974 and was written by Dr. V. V. Liepa.

This report has been assigned Radiation Laboratory Report Number 011764-2-T for internal control purposes, and was submitted by the authors for sponsor approval on 25 March 1974.

This Technical Report has been reviewed and is approved for publication



OLLIE H. EDWARDS  
Colonel, USAF  
Chief, Electronic Warfare Division

## ABSTRACT

This report describes a program that computes the far field scattering pattern of a two-dimensional cylindrical body (or bodies) treated with absorbing materials. The body surface is assumed to satisfy an impedance boundary condition and the absorber is modeled by equivalent electric and magnetic sheets. The program reduces the coupled integral equations governing the surface currents to a system of simultaneous linear equations, solves for the unknown currents, and then computes the far field pattern from the solution. The integral equations derived and presented in a previous interim report were used as the basis for preliminary versions of the program, but these equations have been found to be in error. The required correction consists of incorporating terms previously omitted and the corrected equations are presented and discussed. Careful attention is given to a description of the input data necessary to run the program and the results of a sample run are included for illustration.

The program was developed to explore the effects of absorbent materials on the scattering of electromagnetic waves by edges. Programs used previously in similar explorations embodied a surface impedance boundary condition; for lossy materials covering smooth surfaces of large radius of curvature, such an impedance can be estimated from the layer thickness and material properties, but the relationship breaks down near edges. The program described in this report, however, models the effects of actual materials rather than using the nebulous surface impedance boundary condition.

**MISSING  
PAGE**

## TABLE OF CONTENTS

I	INTRODUCTION	1
II	MATHEMATICAL FORMULATION	4
	2.1 Amended Sheet Equations	4
	2.2 The Required Equations	9
	2.3 Numerical Procedures	13
III	PROGRAM DESCRIPTION	21
IV	LIST OF FORTRAN SYMBOLS	28
V	USER INSTRUCTIONS AND SPECIAL CONSIDERATIONS	31
	5.1 IBM-CDC Compatibility	31
	5.2 Sample Run	32
VI	CONCLUSIONS	45
	APPENDIX: PROGRAM LISTING	47
	REFERENCES	69

# I

## INTRODUCTION

This report describes a computer program (RAMVS) that solves the two-dimensional integral equations for the currents induced upon the surfaces of cylindrical bodies and thin sheets. The fields on the surfaces of solid bodies are assumed to satisfy an impedance boundary condition and the sheets are assumed to be electrically or "magnetically" resistive. Electric and magnetic sheets can be superposed and, if their resistivities are properly chosen, can be used to model the effect of a layer of absorbing material having arbitrary permittivity and permeability. The program reduces the coupled integral equations to a system of simultaneous linear equations, solves for the unknown currents, and from these computes the far field scattering patterns.

RAMVS was developed as a tool to study methods of reducing non-specular scattering and has been used to compute the scattering patterns of simple shapes treated with resistive sheets. As such, it was always a single body that was specified on input. However, the program "understands" only two kinds of surfaces—thin resistive sheets and impedance surfaces—and cannot distinguish between a single body and multiple bodies, as long as all are identified with one class of surface. Thus, although RAMVS has not been used for multiple impedance surface scatterers, it well could have been. Similarly, the program views disjointed resistive sheets as a single surface even though several distinct sheets may be specified on input. These sheets need not be attached to the body or bodies, and in fact the physical separation could be hundreds of wavelengths if, for some reason, such a configuration were of interest.

The program allows the impedances and resistivities to vary from point to point along the profile according to a selection of mathematical distributions provided internally. Metallic bodies and sheets may be modeled by simply specifying a constant surface impedance or resistance of zero. Any combination of sheets and body profiles may be specified on input, but the configuration



must be symmetrical. Only half the profile should be specified because the program generates the other half by imaging about the plane of symmetry ( $y = 0$ ). For running the program on a typical installation ( $\sim 60 K_{10}$  word core), the total perimeter of all surfaces should not exceed ten wavelengths or so. This provides for a sampling rate of 8 or 10 points per wavelength and a maximum of a  $150 \times 150$  element matrix to be solved. Because of coupling between the integral equations, the maximum number of sampling points must include those on the resistive sheets twice; for example, a body having 100 sampling points, in the presence of a sheet with 25, would represent a total of 150 unknown current elements.

RAMVS is based upon the integral equations derived and presented in a previous Interim Report (Knott and Senior, 1974) and the pertinent equations are repeated and rearranged in a form more appropriate for numerical computation. Late in the development of the program, errors were discovered in the previous integral equation formulation, resulting in the omission of some terms. The necessary correction is discussed in Chapter II, and the corrected equations are given. Both the previous and corrected form of the equations contain higher order singularities which require special numerical treatment, and this treatment has been covered in a previous report.

A description of the code is given in Chapter III and provides the reader with an overview of the functioning of each subprogram. For readers who wish to examine the details of the programming, a source listing of RAMVS is given in the Appendix. A list of FORTRAN symbols may be found in Chapter IV to assist the reader in relating the program variables to the mathematical description of the integral equations.

Detailed instructions for the preparation of input data are presented in Chapter V and it is assumed that the user has some familiarity with FORTRAN data formats. The form of the input deck is illustrated by means of a specific example, and the preliminary calculations and decisions that must be made before the deck can be prepared are discussed. The required content of each

card is described and a sample run is displayed to show the results of the program for the specific geometry chosen for illustration.

RAMVS has been successfully run on the IBM 360/67 computer at The University of Michigan and on the CDC 6600 computer at WPAFB. It was tested for special cases, such as isolated impedance bodies and isolated dielectric strips, by means of comparison with other programs that have been verified, as well as with measured data. However, the program has not been thoroughly tested for general, absorber-clad bodies due to the lack of any data for comparison, and the user should be cautious and critical in surveying the computed results for such cases. The authors would appreciate learning about any comparisons of computed results with other data that either demonstrate the program's capability or that show its weaknesses.

## II MATHEMATICAL FORMULATION

We are here concerned with the problem of a plane electromagnetic wave incident on a structure consisting of a cylinder of arbitrary profile in the presence of a generalized resistive sheet of infinitesimal thickness. The entire structure is independent of the  $z$  coordinate of a Cartesian coordinate system  $(x, y, z)$  and the plane wave is incident in the  $xy$  plane with either the electric or magnetic vector in the  $z$  direction, corresponding to E- or H-polarization respectively. The problem is therefore two-dimensional and the geometry is depicted in Fig. 2-1.

The profile of the (closed) cylinder is designated  $C_2$  and here an impedance boundary condition is imposed. The surface impedance  $\eta$  is arbitrary and can vary as a function of position. The resistive sheet profile is designated  $C_1$  and may consist of several disjoint parts, each representing an individual sheet. The boundary conditions at the sheet are specified by the bulk permittivity  $\epsilon_r$ , the bulk permeability  $\mu_r$  and the thickness  $\Delta$  of the material being modelled. Special cases are those of electric or magnetic resistivities alone.

RAMVS is a computer program for the digital solution of the coupled integral equations for the currents induced in the structure, from which the scattered fields are then determined. The integral equations were derived in a previous technical report (Knott and Senior, 1974), but owing to an error, some of the equations presented there are invalid for the type of sheet now considered. We shall therefore begin by detailing the nature of this error.

### 2.1 Amended Sheet Equations

In the study of the integral equations for thin sheets which are electrically or magnetically resistive, or which have an impedance boundary condition imposed at the surface, an analytical error was made in Knott and Senior (1974) which invalidates the results for simple nonplanar sheets and for multi-sheets which are not co-planar.

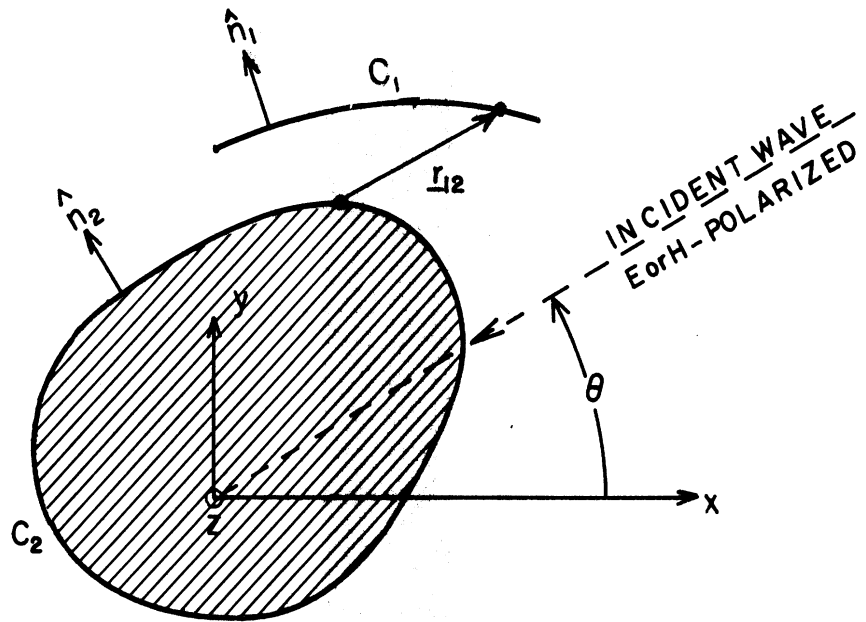


FIG. 2-1: Geometry for the composite scatterer.

- $C_1$ : Absorber sheet, described by  $\epsilon_r, \mu_r$  and the thickness of the material
- $C_2$ : Impedance body described by arbitrary surface impedance  $\eta$ .

The error first appeared in the reduction of eq. (2.24) for a thin impedance boundary condition sheet with H-polarization. Subtraction of the two limits as the observation point  $\rho$  approaches the sheet from above and below does, indeed, produce an identity for  $J_2(s)$ , but on addition we have

$$H_z^i(s) = \frac{1}{2} J_1(s) + \frac{1}{4} \int_{C_+} \eta(s') J_1(s') H_0^{(1)}(kr) d(ks') - \frac{i}{4} \oint_{C_+} J_2(s') (\hat{n}' \cdot \hat{r}) H_1^{(1)}(kr) d(ks'). \quad (2.27'; 2.1)$$

This differs from the equation originally obtained due to the presence of the second integral. As indicated by the slash, this is a Cauchy principal value integral, since the self-cell contributions cancel on summing the limits. Similarly, eq. (2.29) must be replaced by

$$Y_0 E_s^i(s) = \frac{1}{2} \eta(s) J_2(s) + \lim_{\rho \rightarrow C_+} \frac{1}{4k} \frac{\partial}{\partial n} \int_{C_+} J_2(s') (\hat{n}' \cdot \hat{r}) H_1^{(1)}(kr) d(ks') - \frac{i}{4} \oint_{C_+} \eta(s') J_1(s') (\hat{n}' \cdot \hat{r}) H_1^{(1)}(kr) d(ks') \quad (2.29'; 2.2)$$

where the normals are all with respect to the upper surface.

The additional terms in (2.27') and (2.29') vanish identically for a single planar sheet since then  $\hat{n} \cdot \hat{r} = \hat{n}' \cdot \hat{r} = 0$ . In this particular case, eqs. (2.27) and (2.29) are correct as they stand, and are decoupled integral equations for  $J_1(s)$  and  $J_2(s)$  respectively. In all other cases, however, the equations are coupled and both must be solved to determine even the total electric current, proportional to  $J_2(s)$ .

The analogous equations for E-polarization can be obtained using duality and are

$$\begin{aligned}
Y_0 E_z^i(s) = & \frac{1}{2} \eta(s) J_3(s) + \frac{1}{4} \int_{C_+} J_3(s') H_0^{(1)}(kr) d(ks') \\
& - \frac{iY_0}{4} \int_{C_+} J_4(s') (\hat{n}' \cdot \hat{r}) H_1^{(1)}(kr) d(ks')
\end{aligned}
\tag{2.32':2.3}$$

and

$$\begin{aligned}
Z_0 H_s^i(s) = & - \frac{1}{2\eta(s)} J_4(s) - \lim_{\rho \rightarrow C_+} \frac{1}{4k} \frac{1}{\partial n} \int_{C_+} J_4(s') (\hat{n}' \cdot \hat{r}) H_1^{(1)}(kr) d(ks') \\
& + \frac{iZ_0}{4} \int_{C_+} J_3(s') (\hat{n}' \cdot \hat{r}) H_1^{(1)}(kr) d(ks')
\end{aligned}
\tag{2.33':2.4}$$

where

$$J_3(s) = \frac{Y_0}{\eta(s)} (E_z^+ + E_z^-),$$

$$J_4(s) = E_z^+ - E_z^-.$$

The added terms in (2.32') and (2.33') couple the equations, but vanish for a single planar sheet. For this reason, the later equations in Chapter II of Knott and Senior (1974) are correct as they stand.

These same errors recur in Sections 4.2 and 4.3 where generalized (i. e., multiple) resistive sheets are considered, but do not affect any of the equations or discussion through page 33 in Chapter IV. However, eqs. (4.32) and (4.33) for a generalized resistive sheet with E-polarization are in error by the absence of the coupling terms and should read

$$\begin{aligned}
Z_0 H_s^i(s) = Z_0 R^*(s) J_s^*(s) + \lim_{\rho \rightarrow C} \frac{1}{4k} \frac{\partial}{\partial n} \int_C J_s^*(s') (\hat{n}' \cdot \hat{r}) H_1^{(1)}(kr) d(ks') \\
+ \frac{iZ_0}{4} \int_C J_z(s') (\hat{n}' \cdot \hat{r}) H_1^{(1)}(kr) d(ks') \quad ,
\end{aligned}
\tag{4.32':2.5}$$

$$\begin{aligned}
Y_0 E_z^i(s) = Y_0 R(s) J_z(s) + \frac{1}{4} \int_C J_z(s') H_0^{(1)}(kr) d(ks') \\
+ \frac{iY_0}{4} \int_C J_s^*(s') (\hat{n}' \cdot \hat{r}) H_1^{(1)}(kr) d(ks') \quad .
\end{aligned}
\tag{4.33':2.6}$$

These terms must also be introduced into eqs. (4.43) and (4.44) for a generalized resistive sheet in the presence of an imperfectly conducting body, and the equations then become

$$\begin{aligned}
Y_0 E_z^i(s_1) = Y_0 R(s_1) J_z(s_1) + \frac{1}{4} \int_{C_1} J_z(s') H_0^{(1)}(kr_{11}) d(ks') \\
+ \frac{iY_0}{4} \int_{C_1} J_s^*(s') (\hat{n}' \cdot \hat{r}_{11}) H_1^{(1)}(kr) d(ks') + \frac{1}{4} \int_{C_2} K_z(s') H_0^{(1)}(kr_{12}) d(ks') \\
- \frac{i}{4} \int_{C_2} \eta(s') K_z(s') (\hat{n}' \cdot \hat{r}_{12}) H_1^{(1)}(kr_{12}) d(ks') \quad ,
\end{aligned}
\tag{4.43':2.7}$$

$$\begin{aligned}
H_s^i(s_1) = & R^*(s_1)J_s^*(s_1) + \lim_{\rho \rightarrow \rho_1} \frac{Y_0}{4k} \frac{\partial}{\partial n_1} \int_{C_1} J_s^*(s')(\hat{n}' \cdot \hat{r}_{01})H_1^{(1)}(kr_{01})d(ks') \\
& + \frac{i}{4} \int_{C_1} J_z(s')(\hat{n}' \cdot \hat{r}_{11})H_1^{(1)}(kr_{11})d(ks') + \frac{i}{4} \int_{C_2} K_z(s')(\hat{n}' \cdot \hat{r}_{12})H_1^{(1)}(kr_{12})d(ks') \\
& - \frac{i}{4k} \int_{C_2} \eta(s')K_z(s') \frac{\partial}{\partial n_1} \left\{ (\hat{n}' \cdot \hat{r}_{12})H_1^{(1)}(kr_{12}) \right\} d(ks') . \quad (4.44':2.8)
\end{aligned}$$

We note in passing that the incorrect eq. (4.42) is the root of all these errors.

The set of three equations necessary for the complete solution of the problem consists of (4.43'), (4.44') and one of (4.45) and (4.46). For reasons stated previously, the more convenient combination is (4.43'), (4.44') and (4.45). The additional terms in (4.43') and (4.44') vis-a-vis (4.43) and (4.44) vanish if

$$\hat{n} \cdot \hat{r}_{11} = \hat{n}' \cdot \hat{r}_{11} = 0$$

i. e. , all the sheets are co-planar. Until recently, this was the only case where the equations had been studied in detail and numerical data obtained. For a single electrically resistive sheet ( $R^* = \infty$ , implying  $J_s^* \equiv 0$ ) and a perfectly conducting body ( $\eta = 0$ ), eq. (4.43') reduces to (4.47), so that the equations (4.47) and (4.43) used in program REST are not affected by the error.

## 2.2 The Required Equations

The integral equations used in RAMVS for E-polarization are (2.7) and (2.8) above and eq. (4.45) of Knott and Senior (1974). To facilitate the programming, it is convenient to rearrange the equations and to change the notation slightly. The equations then read



$$\begin{aligned}
Y_0 E_z^i(s_1) &= Z_e(s_1) J_z(s_1) + \frac{1}{4} \int_{C_1} J_z(s') H_0^{(1)}(kr) d(ks') \\
&+ \frac{iY_0}{4} \int_{C_1} J_s^*(s') (\hat{n}' \cdot \hat{r}) H_1^{(1)}(kr) d(ks') \\
&+ \frac{1}{4} \int_{C_2} K_z(s') H_0^{(1)}(kr) d(ks') \\
&- \frac{i}{4} \int_{C_2} \eta(s') K_z(s') (\hat{n}' \cdot \hat{r}) H_1^{(1)}(kr) d(ks') \quad , \quad (2.7)
\end{aligned}$$

$$\begin{aligned}
H_s^i(s_1) &= \frac{i}{4} \int_{C_1} J_z(s') (\hat{n}' \cdot \hat{r}) H_1^{(1)}(kr) d(ks') + Z_m(s_1) J_s^*(s_1) \\
&+ \lim_{\rho \rightarrow \rho_1} \frac{Y_0}{4k} \frac{\partial}{\partial n_1} \int_{C_1} J_s^*(s') (\hat{n}' \cdot \hat{r}) H_1^{(1)}(kr) d(ks') \\
&+ \frac{i}{4} \int_{C_2} K_z(s') (\hat{n}' \cdot \hat{r}) H_1^{(1)}(kr) d(ks') \\
&- \frac{1}{4k} \int_{C_2} \eta(s') K_z(s') \frac{\partial}{\partial n_1} \left\{ (\hat{n}' \cdot \hat{r}) H_1^{(1)}(kr) \right\} d(ks') \quad , \quad (2.8)
\end{aligned}$$

$$\begin{aligned}
Y_0 E_Z^i(s_2) = & \frac{1}{4} \int_{C_1} J_Z(s') H_0^{(1)}(kr) d(ks') + \frac{iY_0}{4} \int_{C_1} J_S^*(s') (\hat{n}' \cdot \hat{r}) H_1^{(1)}(kr) d(ks') \\
& + \frac{1}{2} \eta(s_2) K_Z(s_2) + \frac{1}{4} \int_{C_2} K_Z(s') H_0^{(1)}(kr) d(ks') \\
& - \frac{i}{4} \int_{C_2} \eta(s') K_Z(s') (\hat{n}' \cdot \hat{r}) H_1^{(1)}(kr) d(ks') . \tag{2.9}
\end{aligned}$$

The analogous equations for H-polarization can be obtained using duality.

This requires the application of the transformation

$$\begin{aligned}
E_Z^i & \longrightarrow H_Z^i , & H_S^i & \longrightarrow -E_S^i , & Y_0 & \longleftrightarrow Z_0 , \\
J_Z & \longrightarrow J_Z^* , & J_S^* & \longrightarrow -J_S , & \eta & \longrightarrow 1/\eta , \\
K_Z & \longrightarrow K_Z^* = \eta Z_0 K_S , & & & Z_e & \longleftrightarrow Z_m
\end{aligned}$$

to the above equations and gives

$$\begin{aligned}
H_Z^i(s_1) = & Z_m(s_1) Y_0 J_Z^*(s_1) + \frac{Y_0}{4} \int_{C_1} J_Z^*(s') H_0^{(1)}(kr) d(ks') \\
& - \frac{i}{4} \int_{C_1} J_S(s') (\hat{n}' \cdot \hat{r}) H_1^{(1)}(kr) d(ks') + \frac{1}{4} \int_{C_2} \eta(s') K_S(s') H_0^{(1)}(kr) d(ks') \\
& - \frac{i}{4} \int_{C_2} K_S(s') (\hat{n}' \cdot \hat{r}) H_1^{(1)}(kr) d(ks') , \tag{2.10}
\end{aligned}$$

$$\begin{aligned}
-Y_0 E_s^i(s_1) = & -Z_e(s_1) J_s(s_1) + \frac{iY_0}{4} \int_{C_1} J_z^*(s') (\hat{n}' \cdot \hat{r}) H_1^{(1)}(kr) d(ks') \\
& - \lim_{\rho \rightarrow \rho_1} \frac{1}{4k} \frac{\partial}{\partial n_1} \int_{C_1} J_s(s') (\hat{n}' \cdot \hat{r}) H_1^{(1)}(kr) d(ks') \\
& + \frac{i}{4} \int_{C_2} \eta(s') K_s(s') (\hat{n}' \cdot \hat{r}) H_1^{(1)}(kr) d(ks') \\
& - \frac{1}{4k} \int_{C_2} K_s(s') \frac{\partial}{\partial n_1} \left\{ (\hat{n}' \cdot \hat{r}) H_1^{(1)}(kr) \right\} d(ks') \quad , \quad (2.11)
\end{aligned}$$

$$\begin{aligned}
H_z^i(s_2) = & \frac{Y_0}{4} \int_{C_1} J_z^*(s') H_0^{(1)}(kr) d(ks') - \frac{i}{4} \int_{C_1} J_s(s') (\hat{n}' \cdot \hat{r}) H_1^{(1)}(kr) d(ks') \\
& + \frac{1}{2} K_s(s_2) + \frac{1}{4} \int_{C_2} \eta(s') K_s(s') H_0^{(1)}(kr) d(ks') \\
& - \frac{i}{4} \int_{C_2} K_s(s') (\hat{n}' \cdot \hat{r}) H_1^{(1)}(kr) d(ks') \quad . \quad (2.12)
\end{aligned}$$

The three equations in each set are coupled by the unknown currents:  $J_z(s)$  or  $J_s(s)$ , and  $J_s^*(s)$  or  $J_z^*(s)$ , representing the total electric or magnetic currents borne by the resistive sheet, and  $K_z(s)$  or  $K_s(s)$  representing the surface electric current density on the cylinder. The normalized electric and magnetic sheet impedances are defined as

$$Z_e = \frac{i}{2\pi(\epsilon_r - 1)\Delta/\lambda} \quad , \quad (2.13)$$

$$Z_m = \frac{i}{2\pi(\mu_r - 1)\Delta/\lambda} \quad , \quad (2.14)$$

where  $\Delta$  is the thickness of the sheet and  $\lambda$  is the free space wavelength. These parameters are used in preference to the resistivities  $R$  and  $R^*$  of Knott and Senior (1974) since they are of order unity for values of  $\epsilon_r$ ,  $\mu_r$  and  $\Delta/\lambda$  of practical interest. In addition, they are dimensionless and in this respect are compatible with the surface impedance  $\eta$  of the cylinder.

Since the two sets of equations are related via the duality transformation, it is not surprising that the corresponding equations are mathematically similar. We can therefore describe the manner in which the various integrals are handled by using the equations for E-polarization as an example.

### 2.3 Numerical Procedures

To develop the computer code, and especially the sub-programs for generating the matrix elements, it is convenient to write the E-polarized equations as

$$Y_0 E_Z^i(s_1) = A_1 J_Z(s_1) + A_2 J_S^*(s_1) + A_3 K_Z(s_2) \quad , \quad (2.15)$$

$$H_S(s_1) = A_4 J_Z(s_1) + A_5 J_S^*(s_1) + A_6 K_Z(s_2) \quad , \quad (2.16)$$

$$Y_0 E_Z^i(s_2) = A_7 J_Z(s_1) + A_8 J_S^*(s_1) + A_9 K_Z(s_2) \quad , \quad (2.17)$$

where the  $A$ 's are integral operators whose specific forms are evident from eqs. (2.7) through (2.9). Thus, for example,

$$A_1 J_Z(s_1) = Z_e(s_1) J_Z(s_1) + \frac{1}{4} \int_{C_1} J_Z(s') H_0^{(1)}(kr) d(ks') \quad ,$$

$$A_2 J_s^*(s_1) = \frac{iY_0}{4} \oint_{C_1} J_s^*(s') (\hat{n}' \cdot \hat{r}) H_1^{(1)}(kr) d(ks') ,$$

and so on.

The standard practice for evaluating the integrals is to divide each range of integration into segments (or cells) and compute their contributions assuming a specific type of variation of the unknown current over the cells. In prior programs we have, for simplicity, used the elementary "flat-top" approach in which the current is assumed constant over a cell. The contribution from each cell is then proportional to the sampled value of the current at its mid-point. However, several of the integral operators have singular kernels and the "self cell" containing the point of observation then requires individual treatment. For all except one of the singularities, the method that we employ is relatively straightforward, but in the exceptional case, the higher order singularity involved necessitates a special treatment for adjacent cells in addition to the self cell. The reasons for this are described in Knott and Senior (1974; Appendix A) where the details of the treatment can be found.

We now examine in turn each of the integral operators  $A_1$  through  $A_9$  and show how the numerical computations are performed. The kernel of the operator  $A_1$  has a logarithmic singularity, and by approximating the zero order Hankel function, the self cell contribution can be evaluated analytically. The result is

$$A_1 J_z(s_1) = \left\{ Z_e(s_1) + \frac{\Delta(s_1)}{\lambda} \left[ \frac{\pi}{2} + i \left( \ln \frac{\Delta(s_1)}{\lambda} + 0.02879837 \right) \right] \right\} J_z(s_1) \\ + \int_{\pm 2\Delta} J_z(s') H_0^{(1)}(kr) d(ks') + \int_{C_1 - (\Delta \mp 2\Delta)} J_z(s') H_0^{(1)}(kr) d(ks') , \quad (2.18)$$

where the bracketed terms represent contributions by the self cell. The first integral on the right side is evaluated using a three-point Simpson's rule

$$\int_a^b f(x)dx = \frac{b-a}{6} \left\{ f(a) + 4f\left(\frac{a+b}{2}\right) + f(b) \right\}$$

and the integral over  $C_1 - (\Delta \pm 2\Delta)$  represents the contribution from the remainder of the surface  $C_1$ . The integral is actually coded as a discrete summation over all the cells  $i \neq j$ , but we have found it just as convenient (and less confusing) to refer to it as an integral in the coding process.

The integral in  $A_2$  is a Cauchy principal value, and has no self cell.

Since

$$H_1^{(1)}(kr) = -\frac{\partial}{\partial(kr)} H_0^{(1)}(kr) \quad \text{and} \quad \frac{\partial}{\partial(kr)} = (\hat{s}' \cdot \hat{r}) \frac{\partial}{\partial(ks')}$$

$$A_2 J_s^*(s_1) = \frac{iY_0}{4} \int_{C_1 - \Delta} J_s^*(s') (\hat{n}' \cdot \hat{r}) H_1^{(1)}(kr) d(ks')$$

can be reduced to the form

$$\begin{aligned} A_2 J_s^*(s_1) = & -\frac{iY_0}{4} \int_{\pm 2\Delta} \left| J_s^*(s') (\hat{n}' \cdot \hat{r}) (\hat{s}' \cdot \hat{r}) \frac{\partial}{\partial(ks')} \left\{ H_0^{(1)}(kr) \right\} \right| d(ks') \\ & + \frac{iY_0}{4} \int_{C_1 - (\Delta \mp 2\Delta)} J_s^*(s') (\hat{n}' \cdot \hat{r}) H_1^{(1)}(kr) d(ks') . \end{aligned} \quad (2.19)$$

The first integral is evaluated over each cell as

$$-\frac{iY_0}{4} J_s^*(s_j) (\hat{n}_j \cdot \hat{r}_{ij}) (\hat{s}_j \cdot \hat{r}_{ij}) H_0^{(1)}(kr) \Big|_{a(\Delta_j)}^{b(\Delta_j)} ,$$

where  $a(\Delta_j)$  and  $b(\Delta_j)$  are the endpoints of the source cell  $j$ , and the second integral is evaluated as in (2.18).

In  $A_3$  the integration is over the surface  $C_2$  with the observation point on  $C_1$ . There is again no self cell and the integral

$$A_3 K_Z(s_2) = \frac{1}{4} \int_{C_2} K_Z(s') \left\{ H_0^{(1)}(kr) - i\eta(s')(\hat{n}' \cdot \hat{r}) H_1^{(1)}(kr) \right\} d(ks') \quad (2.20)$$

can be evaluated directly. The operator

$$A_4 J_Z(s_1) = \frac{i}{4} \int_{C_1 - \Delta} J_Z(s') (\hat{n}' \cdot \hat{r}) H_1^{(1)}(kr) d(ks')$$

is treated similarly to  $A_2$ , giving

$$\begin{aligned} A_4 J_Z(s_1) = & -\frac{i}{4} \int_{\pm 2\Delta} J_Z(s') (\hat{n}' \cdot \hat{r}) (\hat{s}' \cdot \hat{r}) \frac{\partial}{\partial(ks')} \left\{ H_0^{(1)}(kr) \right\} d(ks') \\ & + \frac{i}{4} \int_{C_1 - (\Delta \mp 2\Delta)} J_Z(s') (\hat{n}' \cdot \hat{r}) H_1^{(1)}(kr) d(ks') . \end{aligned} \quad (2.21)$$

The singularity in

$$A_5 J_S^*(s_1) = Z_m(s_1) J_S^*(s_1) + \lim_{\rho \rightarrow \rho_1} \frac{Y_0}{4k} \frac{1}{\partial n_1} \int_{C_1} J_S^*(s') (\hat{n}' \cdot \hat{r}) H_1^{(1)}(kr) d(ks') ,$$

however, is the most difficult one. The differentiation with respect to the normal effectively increases (by  $1/r$ ) the order of the singularity of the kernel, but since the same type of operator also occurs in the integral equation for an electrically resistive sheet with H-polarization, we can use the representation previously developed (Knott and Senior, 1974) for that equation. We then have

$$\begin{aligned}
A_5 J_s^*(s_1) = & \left\{ Z_m(s_1) + \frac{iY_0}{2\pi\Delta/\lambda} + Y_0 \frac{\Delta(s_1)}{\lambda} \left[ \frac{\pi}{2} + i \left( \ell_n \frac{\Delta(s_1)}{\lambda} + 0.02879837 \right) \right] \right\} J_s^*(s_1) \\
& + \frac{Y_0}{4} \int_{\pm 2\Delta} J_s^*(s') \left\{ (\hat{n}' \cdot \hat{n}) H_0^{(1)}(kr) + \frac{\partial}{\partial(kr)} \left[ (\hat{s} \cdot \hat{r}) H_1^{(1)}(kr) \right] \right\} d(kr) \\
& + \frac{Y_0}{4} \int_{C_1 - (\Delta \mp 2\Delta)} J_s^*(s') \left\{ (\hat{n}' \cdot \hat{r}) (\hat{n} \cdot \hat{r}) H_0^{(1)}(kr) \right. \\
& \left. + \left[ (\hat{s}' \cdot \hat{r}) (\hat{s} \cdot \hat{r}) - (\hat{n}' \cdot \hat{r}) (\hat{n} \cdot \hat{r}) \right] \frac{H_1^{(1)}(kr)}{kr} \right\} d(kr) , \quad (2.22)
\end{aligned}$$

where the terms in brackets are produced by the self cell, the next integral is the contribution from the two adjoining cells on either side of the self cell and the last integral is the contribution from the remainder of  $C_1$ . In the computer code the first and third parts on the right side of (2.22) are programmed as shown, but the second part is expanded further. The contribution of a single source cell  $\Delta_j$  to an observation cell  $\Delta_i$ ,  $i \neq j$ , can be written as

$$\frac{Y_0}{4} J_s^*(s_j) (\hat{n}_j \cdot \hat{n}_i) \int_{\Delta_j} H_0^{(1)}(kr) d(kr) + \frac{Y_0}{4} J_s^*(s_j) (\hat{s}_i \cdot \hat{r}_{ij}) H_1^{(1)}(kr) \left. \begin{array}{l} b(\Delta_j) \\ a(\Delta_j) \end{array} \right\} , \quad (2.23)$$

where  $a(\Delta_j)$  and  $b(\Delta_j)$  are the endpoints of the  $j$ th cell. The integral over  $\Delta_j$  is evaluated by a three-point Simpson's rule.

The operator  $A_6$  is relatively simple since the observation point is on  $C_1$  and the source point on  $C_2$ . Only the derivative factor needs expansion and this gives

$$\begin{aligned}
A_6 K_z(s_2) = & -\frac{1}{4k} \int_{C_2} \eta(s') K_z(s') \left\{ (\hat{n}' \cdot \hat{r}) (\hat{n} \cdot \hat{r}) H_0^{(1)}(kr) \right. \\
& \left. + \left[ (\hat{s}' \cdot \hat{r}) (\hat{s} \cdot \hat{r}) - (\hat{n}' \cdot \hat{r}) (\hat{n} \cdot \hat{r}) \right] \frac{H_1^{(1)}(kr)}{kr} \right\} d(kr) . \quad (2.24)
\end{aligned}$$



The operators  $A_7$  and  $A_8$  are programmed without modification:

$$A_7 J_z(s_2) = \frac{1}{4} \int_{C_1} J_z(s') H_0^{(1)}(kr) d(ks') , \quad (2.25)$$

$$A_8 J_s^*(s_2) = \frac{iY_0}{4} \int_{C_1} J_s^*(s') (\hat{n}' \cdot \hat{r}) H_1^{(1)}(kr) d(ks') , \quad (2.26)$$

and with the final operator  $A_9$ , the self cell contribution must be removed from the first of the two integrals. The procedure is directly analogous to that for  $A_1$  and yields

$$A_9 K_z(s_2) = \left\{ \frac{1}{2} \eta(s_2) + \frac{\Delta(s_2)}{\lambda} \left[ \frac{\pi}{2} + i \left( \ln \frac{\Delta(s_2)}{\lambda} + 0.02879837 \right) \right] \right\} K_z(s_2) \\ + \frac{1}{4} \int_{C_2^{-\Delta}} K_z(s') \left\{ H_0^{(1)}(kr) - i\eta(s') (\hat{n}' \cdot \hat{r}) H_1^{(1)}(kr) \right\} d(ks') . \quad (2.27)$$

The expressions for the far field scattering can be deduced from eqs. (2.7) and (2.9) for E-polarization and (2.10) and (2.12) for H-polarization by replacing the Hankel functions by their asymptotic expansions for large argument. Each of these four equations has the form

$$F_z^i = F_z^t - F_z^s$$

where  $F$  represents either  $Y_0 E_z$  or  $H_z$  depending on the polarization and the superscript  $t$  denotes the total field. Since  $F_z^s$  is simply the negative of the integral terms in the equations, a far field value can be obtained by selecting those integrals representing  $C_2$  contributions observed on  $C_1$  or  $C_1$  contributions observed on  $C_2$ . It then follows that for E-polarization

$$\begin{aligned}
Y_0 E_z^s(\rho, \theta) &\sim \sqrt{\frac{2}{\pi k \rho}} e^{ik\rho - i\frac{\pi}{4}} \frac{1}{4} \left\{ - \int_{C_1} J_z(s') e^{-ik(x' \cos \theta + y' \sin \theta)} d(ks') \right. \\
&- Y_0 \int_{C_1} J_s^*(s') (\hat{n}' \cdot \hat{r}) e^{-ik(x' \cos \theta + y' \sin \theta)} d(ks') \\
&\left. - \int_{C_2} K_z(s') \{1 - \eta(s') (\hat{n}' \cdot \hat{r})\} e^{-ik(x' \cos \theta + y' \sin \theta)} d(ks') \right\}, \quad (2.28)
\end{aligned}$$

and for H-polarization

$$\begin{aligned}
H_z^s(\rho, \theta) &\sim \sqrt{\frac{2}{\pi k \rho}} e^{ik\rho - i\frac{\pi}{4}} \frac{1}{4} \left\{ - Y_0 \int_{C_1} J_z^*(s') e^{-ik(x' \cos \theta + y' \sin \theta)} d(ks') \right. \\
&+ \int_{C_1} J_s(s') (\hat{n}' \cdot \hat{r}) e^{-ik(x' \cos \theta + y' \sin \theta)} d(ks') \\
&\left. - \int_{C_2} K_s(s') \{\eta(s') - (\hat{n}' \cdot \hat{r})\} e^{-ik(x' \cos \theta + y' \sin \theta)} d(ks') \right\}, \quad (2.29)
\end{aligned}$$

where  $\theta$  is the scattering direction measured anticlockwise from the positive  $x$  axis and  $\hat{r}$  is a unit vector to the observation point.

The two-dimensional scattering cross sections are

$$\frac{\sigma(\theta, \phi)}{\lambda} = \lim_{\rho \rightarrow \infty} \frac{2\pi\rho}{\lambda} \left| \frac{Y_0 E_z^s(\theta, \phi)}{Y_0 E_z^i(\phi)} \right|^2 \quad (2.30)$$

and

$$\frac{\sigma(\theta, \phi)}{\lambda} = \lim_{\rho \rightarrow \infty} \frac{2\pi\rho}{\lambda} \left| \frac{H_Z^s(\theta, \phi)}{H_Z^i(\phi)} \right|^2 \quad (2.31)$$

where  $\phi$  is the angle of incidence. These show why it is convenient to choose

$$\left| Y_0 E_Z^i(\theta) \right| = \left| H_Z^i(\theta) \right| = 1 \quad .$$

### III PROGRAM DESCRIPTION

RAMVS is based in eqs. (2.7) through (2.12) and uses the particular mathematical expansions given by eqs. (2.18) through (2.31). There are three variables to be determined: the total electric and magnetic currents  $\underline{J}$  and  $\underline{J}^*$ , respectively, carried by the absorber sheet, and a surface current  $\underline{K}$  on the impedance surface. If  $M$  is the number of cells used for the absorber sheet, and  $K$  is the number of cells used on the impedance surface, the total number of unknowns, and hence the number of linear simultaneous equations to be solved, is  $2M+K$ . This is (approximately) thrice the unknowns encountered in cross section computations for impedance cylinders (program RAMD) or resistive sheets (program REST). (RAMD is discussed by Knott and Senior (1974) and REST by Knott et al. (1973).) It is therefore important that in developing program RAMVS consideration is given to writing a program with the least abuse of computer core space.

Dimensioning has been simplified by structuring the program in modules, with MAIN used only for starting the program and allocating core space. The user of the program must provide appropriate dimensioning only in MAIN.\*

The FORTRAN source program consists of 11 modules (a MAIN program and 10 subprograms) and contains about 850 statements, including comment cards. The structure of the program is shown in Fig. 3-1, where each block represents a particular module. The arrows joining these blocks refer to a typical execution sequence, discussed in the latter part of this section. The

---

\* When linear vectors are dimensioned in the MAIN program and are passed as arguments in the subroutine calling sequence, the dimension of the vector in the subroutine is arbitrary. For two-dimensional vectors, the size of the first dimension entry is passed in the calling sequence along with the vector, while the second entry is arbitrary. Thus in program RAMVS the dimension statements occurring in subroutines are of the form  $A(1)$  or  $B(M, 1)$ .

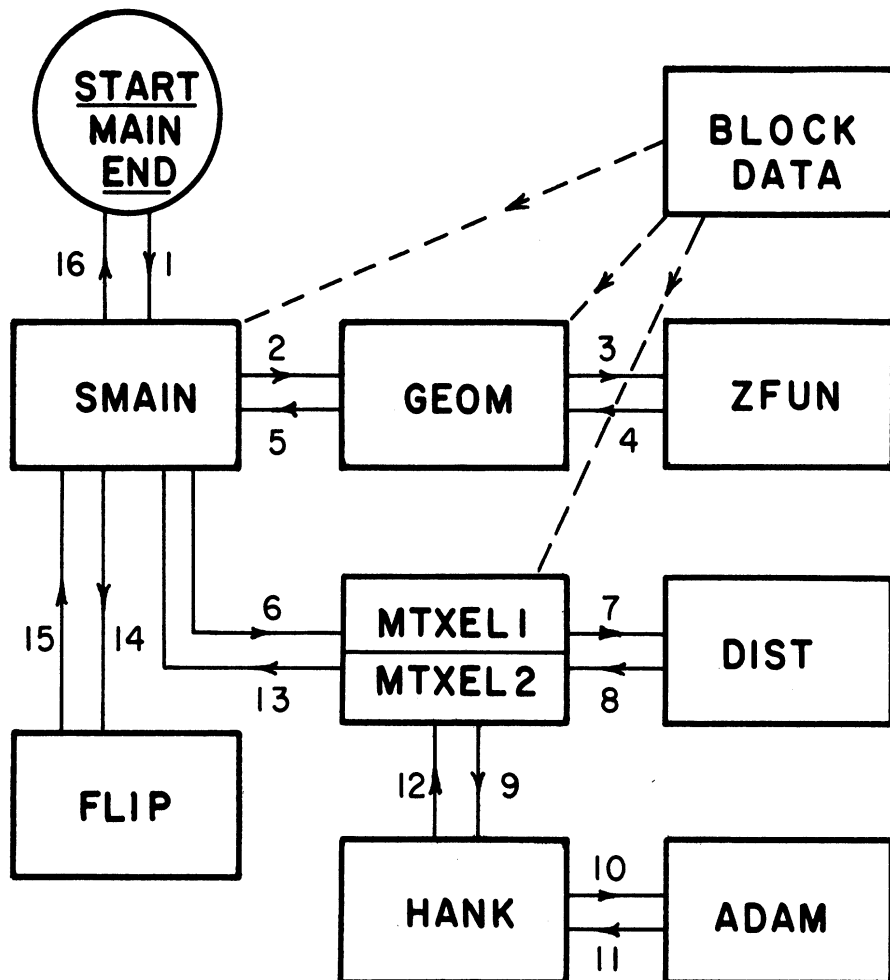


FIG. 3-1: Block diagram and flow graph for the program.

purpose of the modules is as follows.

MAIN This is a short program (7 FORTRAN statements) and its sole purpose is to start the program and allocate the core space for the dominant vectors (dimensioning of arrays). Whenever vectors must be redimensioned, only the MAIN program need be changed.

SUBROUTINE SMAIN MAIN calls subroutine SMAIN, a control program that also performs other operations. These include the reading of control statements, the setting of appropriate controls for the type of computation required, and the calling of various subroutines. SMAIN calls a subroutine GEOM for computation of geometrical and electrical parameters of the scatterer, then calls subroutine MTXEL to generate the matrix and calls subroutine FLIP to invert the matrix and compute the unknown (current) vector. Computations of scattering cross sections and the printing of most of the output is also done in SMAIN.

SUBROUTINE GEOM GEOM, as the name implies, reads the input data specifying the geometry and the electrical characteristics of the scatterer and from these generates point-by-point descriptions of the body required for solving the integral equations. The computations include the position of each cell, the components of the surface normal, the cell width, and the electrical parameters for the cell.

The technique used for reading in the data is the same as used in our other two-dimensional scattering programs, such as RAMD and REST, developed under this contract. It is assumed that the profile of a two-dimensional scatterer can be described by an assembly of circular arcs (a line segment is an arc of very large radius) and that the body is symmetric about the plane  $y = 0$ . Thus, it is sufficient to specify only half of the body and let the computer generate the image. For the special case of a horizontal line (strip) lying in the  $y = 0$  plane, no image is generated.

In GEOM a segment of circular arc is specified by the coordinates of the endpoints and the angle subtended by the arc as measured at the center of the generating circle. While cell coordinates and other parameters are being found, a running distance along the surface is also computed for each line segment.

This distance is used as an independent variable in establishing the surface impedance or absorber sheet impedance distributions along the surface.

COMPLEX FUNCTION ZFUN This subprogram computes a surface impedance distribution according to one of the following mathematical relations:

$$\begin{aligned} Z &= (a - bs)^c, \quad * \\ Z &= a + bs^c, \\ Z &= a + b e^{-cs}, \end{aligned}$$

where  $a$  and  $b$  are complex constants and  $c$  is a real constant. The distance along the surface of the line segment is zero at the first (input) endpoint and increases toward the other. Thus, if the left-most endpoint of a line segment is read in first, the distance is computed from left-to-right or, if the right-most endpoint is read in first, the distance is computed from right-to-left along the particular segment. This adds additional flexibility to the possible impedance variations available from the three expressions given above.

SUBROUTINE MTXEL1 AND SUBROUTINE MTXEL2 Once the geometrical and electrical parameters have been furnished by GEOM and ZFUN for each cell position, matrix elements are generated either by MTXEL1 or MTXEL2, depending on whether the incident wave is E- or H-polarized, respectively. The two subroutines are quite similar structurally, and in the earlier development of the code a single subroutine was used with numerous IF statements to differentiate between the two polarizations. The resultant program was elegant but confusing, and for the sake of simplicity and computational efficiency, the subroutine was replaced by two separate codes.

In typical numerical solutions of electromagnetic scattering and antenna problems, the matrix possesses certain symmetries that can be exploited in the matrix generation, and even in solving for the unknown vector. In the process of development of RAMVS, various computational possibilities were examined that

---

\* In the FORTRAN code this equation is written as  $Z = \exp [c \cdot \log_e (a - bs)]$ .

would reduce the core storage and the computational time. Because of the coupled integral equations which are involved here, the matrix defined by eqs. (2.15) through (2.17) does not, in general, have explicit symmetries associated with typical scatterers that could be readily exploited to save appreciable machine time. To keep the code relatively simple and to reduce programming errors, the matrix elements are computed in a relatively straightforward fashion, with the following modification. Since the electric and the magnetic sheets are physically superimposed and therefore have the same geometrical parameters, the computation of radii between the cells, the Hankel functions, and the dot products need not be duplicated. If  $A$  is the entire matrix and  $A_1, \dots, A_9$  the submatrices as defined in Chapter II, the matrix elements are computed simultaneously in  $A_1, A_2, A_4$  and  $A_5$ , in  $A_3$  and  $A_6$ , and in  $A_7$  and  $A_8$ .

SUBROUTINE DIST Subroutine DIST is called by MTXEL1(2) to compute the distance between the source and observation points (cells) and five kinds of dot products, such as  $(\hat{n} \cdot \hat{r})$ . To save unnecessary computations, one of the arguments in the subroutine calling sequence specifies the particular things to be computed. Thus if the computation of a particular matrix element requires the distance  $r$  between two cells and  $(\hat{n} \cdot \hat{r})$ , only the two are computed by the subroutine.

SUBROUTINE HANKC The generation of matrix elements requires Hankel functions of the first kind, and these are computed in HANKC, complemented by subroutine ADAM. For computations of  $H_0^{(1)}(x)$  and  $H_1^{(1)}(x)$ , HANKC uses polynomial approximations for  $J_0(x)$  and  $Y_0(x)$ ,  $J_1(x)$  and  $Y_1(x)$  (Abramowitz and Stegun, 1964). For the sake of efficiency, one of the arguments in the calling sequence specifies whether  $H_0^{(1)}(x)$  or  $H_1^{(1)}(x)$  is to be computed, or both.

SUBROUTINE ADAM The subroutine ADAM complements HANKC and is used to simplify the code of HANKC.

SUBROUTINE FLIP As the name indicates, this is a matrix inversion subroutine and is an outgrowth of subroutine ZVO8 used in program RAM1A originally supplied to us by AFAL. The technique used is the standard Gauss-Jordan method (IBM, 1966) and the procedure has been explained in detail by



Oshiro (1963). During the inversion process the original matrix  $A$  is replaced by its inverse  $A^{-1}$  and subsequently the solution vector (current vector) is obtained by multiplying  $A^{-1}$  by the excitation field. When a new excitation field is given, matrix inversion is by-passed and the solution vector obtained by multiplying  $A^{-1}$  by the new field.

BLOCK DATA Numerical constants commonly used in RAMVS are stored in COMMON BLOCK. These constants include  $Y_0$ ,  $\pi$ , degree-to-radian conversion factor, and others.

A typical computation cycle in RAMVS is as follows.

MAIN starts the cycle by allocating core space and calling subroutine SMAIN (1)\*. SMAIN, in the first go-around, reads the first three data cards containing a title card and control information, such as incident polarization, bistatic or backscattering cross section to be computed, and others (cards A, B, C, as described in Chapter V). Then GEOM (2) is called, and it reads data specifying geometrical and electrical parameters of the scatterer (cards D through H) which include information such as type of surface, number of cells per segment and type of impedance variation along the surfaces. Using these data, GEOM generates all of the required geometrical parameters and, with help from ZFUN (3,4), the electrical parameters for each cell. Matrix elements are generated next (5,6), either in MTXEL1 or MTXEL2, depending upon the polarization desired. MTXEL first calls DIST (7,8) to compute the distances and various dot products associated with each observation and source point, and then calls on HANKC plus ADAM (9, 10, 11, 12) for the related Hankel function.

Control returns to SMAIN where the incident field vector is computed (13), whereupon FLIP is called (14) to invert the matrix and return (15) the solution vector. SMAIN prints out the geometrical and electrical parameters associated with each cell, along with the current. It then computes either the bistatic or backscattering cross section, and prints out the results. In the case of back-

---

\* Numbers in parentheses indicate the position on the flow-graph in Fig. 3-1.

scattering, FLIP is called (14) to calculate the new current for each new incident direction, and FLIP in turn acknowledges (15) by multiplying the previously computed matrix  $A^{-1}$  by the incident vector.

If additional sets of data are provided, the cycle (2, 3, . . . , 15) is repeated, otherwise the program returns to MAIN (16) and execution is terminated.

## IV

## LIST OF FORTRAN SYMBOLS

This list contains symbols that have been assigned a specific meaning in the program. Words marked by an asterisk are used as prefixes (suffixes) to indicate a particular modification to another variable. Input parameters are also included in this list.

<u>FORTRAN Entry</u>	<u>Description</u>
A(I, J)	Matrix A or its inverse $A^{-1}$
AA	Dummy variable (complex)
AMP*	Usually indicates amplitude
ANG	Angle subtended by an arc segment
BJ	Bessel function $J_{0,1}(x)$
BY	Bessel function $Y_{0,1}(x)$
DIG	Radians-to-degrees conversion factor
DSQ(J)	Cell size
FAC*	Multiplication factor
FIRST	Initial angle of incidence
FORM	Control selects type of impedance variation desired
HONE, H1	Hankel function, $H_1^{(1)}(x)$
HZERO, HZ	Hankel function, $H_0^{(1)}(x)$
I	Index, normally assigned to observation point
ID	Title, "A" format
INK	Angular increment for back/bistatic scattering angles
IAT	Control in subroutine FLIP If IAT = 1, invert matrix If IAT = 2, bypass inversion
II	Index, associated with I

J	Index, usually assigned to source point
JJ	Index, associated with J
K	Number of cells on impedance surface
KODE	Bistatic/backscattering control
L	Index assigned to geometry segment
LAST	Final (last) angle of incidence
LL(I)	A vector in FLIP subroutine
LUMP(2, I)	Array used for cell identification
M	Number of cells on absorber surface
MI	Dimension integer passed to FLIP
MK	$M + K$
M1	$M + 1$
MM1	$M + M + 1$
MMK	$M + M + K$
MORE	Control integer in input data
NDNP	$\hat{n} \cdot \hat{n}'$
NDR	$\hat{n} \cdot \hat{r}$
NPDR	$\hat{n}' \cdot \hat{r}$
PHASE*	Phase of a complex number
PHI(I)	Current vector to be determined
PI	$\pi$
PINK(I)	Excitation vector
PIPI	$\pi \cdot \pi$
PIT	$\pi/2$
P(WAVE)*	P refers to previous value (of wave)
R	$R =  \vec{r}_i - \vec{r}_j $
RED	Degrees-to-radians conversion factor
RK	$2\pi R$
S	Distance along the surface

SDR	$\hat{s} \cdot \hat{r}$
SPDR	$\hat{s}' \cdot \hat{r}$
SUM*	Sum, as the name indicates (complex)
TPI	$2\pi$
WAVE	Incident wavelength
X(I)	x-coordinate of the cell
XA	x-coordinate for first endpoint of an input arc segment
XB	x-coordinate for second endpoint of an input arc segment
XN(I)	x-component of normal vector, $\hat{n}$
Y(I)	y-coordinate of the cell
YA	y-coordinate for first endpoint of an input arc segment
YB	y-coordinate for second endpoint of an input arc segment
YN(I)	y-component of normal vector, $\hat{n}$
YZ	$Y_0$
ZE(I)	Electric impedance vector; ZS(I) is stored in part of ZE(I)
ZEA } ZEB } ZEX }	Coefficients used in ZFUN for computation of ZE(I)
ZM(I)	Magnetic impedance vector
ZMA } ZMB } ZMX }	Coefficients used in ZFUN for computation of ZM(I)
ZSA } ZSB } ZSX }	Coefficients used in ZFUN for computation of surface impedance and stored in vector ZE(I)
ZS	Surface impedance constant

## USER INSTRUCTIONS AND SPECIAL CONSIDERATIONS

The program RAMVS solves the integral equations for currents and bistatic or monostatic scattering from a general two-dimensional body consisting of a closed cylindrical surface with specified surface impedance ZS (stored in ZE) and absorber sheets that are specified by their electric and magnetic sheet resistances (impedances). Mathematical modeling requires that these sheets be thin, and comparison of computed and measured backscattering has shown that for a dielectric sheet reasonable results are obtained when the sheet is as thick as  $0.1\lambda$ , where  $\lambda$  is the free-space wavelength. If thicker sheets are desired, they can be simulated by two or more equivalent thin sheets, requiring, of course, more sampling points.

The size of the body or the number of sampling points that can be used depends on the core size of the machine and the funds or computer time available. If K is the number of sampling points on the impedance surface and M is the number of sampling points on the absorber sheet, the total number of unknowns to be determined is  $2M+K$ .

To assist a potential user intending to run RAMVS, we illustrate the preparation of input data for a hypothetical computation. Partial output for the same data is also presented.

### 5.1 IBM-CDC Compatibility

The program has been compiled and run on the University of Michigan IBM 360/67 computer and the AFAL CDC 6600 machine at WPAFB. Only one discrepancy occurs, and this is in statement 13 (IBM version) in subroutine SMAIN. Depending upon the machine used to run the program, the following (or equivalent) forms should be used:

<u>IBM</u>	<u>CDC</u>
5 READ(5, 100, END=998)ID	5 READ(5, 100)ID IF(EOF(5)) 999, 998 998 CONTINUE

## 5.2 Sample Run

Consider a relatively thin perfectly conducting ogival cylinder to which are attached an absorber fin at the front and two fins at the back. We choose the body to be one wavelength long with its surface generating arc encompassing  $25^\circ$ . The fins are made of material characterized by (complex) permittivity  $\epsilon_r = 5.0 + i3.0$  and permeability  $\mu_r = 2.0 + i1.0$ , and the thickness of the material is 0.05 wavelength. The details of the geometry are shown in Fig. 5-1.

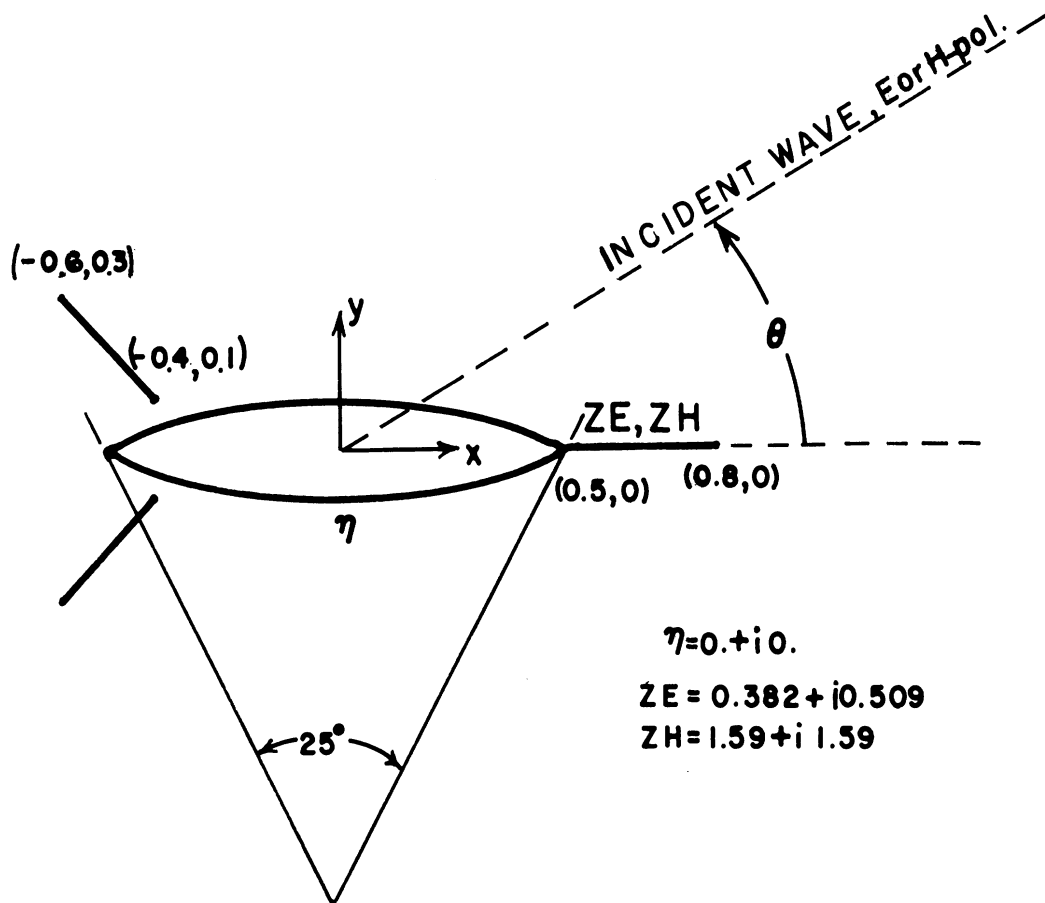


FIG. 5-1: Geometry used in the sample computation.

It is required to compute the backscattering cross section pattern at aspect angles spaced 10 degrees apart for both incident polarizations.

Preliminary computation:

$$Z_E = \frac{i}{2\pi(\epsilon_r - 1)\Delta/\lambda} = \frac{i}{2\pi(4.0 + i3.0)(.05)} = 0.382 + i0.509$$

$$Z_M = \frac{i}{2\pi(\mu_r - 1)\Delta/\lambda} = \frac{i}{2\pi(1.0 + i1.0)(.05)} = 1.59 + i1.59$$

$$Z_S = 0. + i0. \text{ (perfectly conducting) .}$$

Number of sampling points:

Using the criterion of approximately 10 sampling points per free space wavelength, we choose:

- 10 points on each of the upper and lower halves of the ogival cylinder,
- 3 points on the front fin, and
- 3 points on each of the rear fins.

Dimensioning:

If the program is used as listed in the Appendix, the array dimensions are more than adequate. On the other hand, if larger or smaller arrays are desired, the following guidelines should be applied:

- (a) Dimensioning need be changed only in the MAIN program.
- (b) Estimate the number of sampling points that will be used on impedance and absorber surfaces.
- (c) Determine the dimensions of arrays from the following formula:

If  $K$  = number of points on the impedance surface

and  $M$  = number of points on the absorber sheet,

then the pertinent values  $MK$  and  $MMK$  that must be entered in the MAIN program are

$$MK = M + K \quad \text{and} \quad MMK = M + M + K .$$

For particular details, see the comments at the beginning of the program listing (Appendix).



Input data formats:

Below are the input data formats for the RAMVS program. The letters assigned to each format do not necessarily represent the order of the data cards. Depending upon the geometry used and the computational requirements, some formats may be repeated and others not used at all.

*** INPUT DATA FORMAT ***	
A	FORMAT (18A4) TITLE CARD: USE UP TO 72 COLUMNS
B	FORMAT (I2,I3,4F10.5) MORE,IPOL,WAVE,ZSFAC,ZEFAC,ZMFAC MORE=0 THIS WILL BE THE LAST RUN FOR THIS DATA SET MORE=1 THERE ARE MORE DATA TO BE READ AFTER THIS SET IPOL=1 E-POLARIZATION IPOL=2 H-POLARIZATION WAVE WAVELENGTH ZSFAC MULTIPLYING FACTOR (REAL) FOR ALL ZS ZEFAC MULTIPLYING FACTOR (REAL) FOR ALL ZE ZMFAC MULTIPLYING FACTOR (REAL) FOR ALL ZM
C	FORMAT (I2,3X,3F10.5) KODE,FIRST,LAST,INK KODE=0 COMPUTES BISTATIC SCATTERING PATTERN KODE=1 COMPUTES BACKSCATTERING PATTERN FIRST INITIAL SCATTERING AND INCIDENCE ANGLE LAST FINAL ANGLE INK ANGULAR INCREMENT
(DATA D, E, AND F REQUIRED FOR EACH ABSORBER SEGMENT; AT LEAST ONE ABSORBER AND ONE IMPEDANCE SEGMENT IS REQUIRED. ABSORBER SEGMENTS MUST BE READ IN FIRST.)	
D	FORMAT (I2,I3,5F10.5) TYPE,N,XA,YA,XB,YB,ANG TYPE=1 ABSORBER SHEET TYPE=2 IMPEDANCE SURFACE N NUMBER OF SAMPLING POINTS ON THIS SEGMENT XA,YA,XB,YB SEGMENT ENDPOINTS ANG ANGLE SUBTENDED BY THE SEGMENT
E	FORMAT (I2,3X,5F10.5) FORM,ZEA,ZEB,ZEX FORM=-1 $ZE(I)=(ZEA-ZEB*S(I))*ZEX$ FORM= 0 $ZE(I)=ZEA+ZEB*S(I)*ZEX$ FORM= 1 $ZE(I)=ZEA+ZEB*EXP(-ZEX*S(I))$ ZEA,ZEB COMPLEX IMPEDANCE CONSTANTS ZEX REAL IMPEDANCE CONSTANT

F	FORMAT (I2,3X,5F10.5) FORM,ZMA,ZMB,ZMX FORM=-1 ZM(I)=(ZMA-ZMB*S(I))**ZMX FORM= 0 ZM(I)=ZMA+ZMB*S(I)**ZMX FORM= 1 ZM(I)=ZMA+ZMB*EXP(-ZMX*S(I)) ZMA,ZMB COMPLEX IMPEDANCE CONSTANTS ZMX REAL IMPEDANCE CONSTANT
(DATA G AND H REQUIRED FOR EACH IMPEDANCE SEGMENT.)	
G	FORMAT (I2,I3,5F10.5) TYPE,N,XA,YA,XB,YB,ANG TYPE=1 ABSORBER SHEET TYPE=2 IMPEDANCE SURFACE N NUMBER OF SAMPLING POINTS ON THIS SEGMENT XA,YA,XB,YB SEGMENT ENDPOINTS ANG ANGLE SUBTENDED BY THE SEGMENT
H	FORMAT (I2,3X,5F10.5) FORM,ZSA,ZSB,ZSX FORM=-1 ZS(I)=(ZSA-ZSB*S(I))**ZSX FORM= 0 ZS(I)=ZSA+ZSB*S(I)**ZSX FORM= 1 ZS(I)=ZSA+ZSB*EXP(-ZSX*S(I)) ZSA,ZSB COMPLEX IMPEDANCE CONSTANTS ZSX REAL IMPEDANCE CONSTANT
I	FORMAT (I5) INTEGER ZERO IN COLUMN 5 SHUTS OFF READING OF SEGMENT PARAMETERS
(USE THIS CARD ONLY IF, IN B, MORE=1)	
J	FORMAT (I2,I3,4F10.5) MORE,IPOL,WAVE,ZSFAC,ZEFAC,ZMFAC

#### Input data cards:

The data set may consist of as few as 9 cards but can be many more, depending upon the number of segments used to specify the geometry, the number of polarizations and frequencies desired, and the number of constant multiplication factors for the impedances. The geometry must always consist of two surfaces, an impedance surface and an absorber sheet, though either may consist of only two cells far removed from the main scatterer. The data and explanation follows.

(card)	2	5	10	20	30	40	50 (column)
1							
2	1	2	1.	1.	1.	1.	
3	1	1	0.	180.	10.		
4	1	3	0.5	0.	0.8	0.	0.
5	0		0.382	0.509	0.	0.	0.
6	0		1.59	1.59	0.	0.	0.
7	1	3	-0.4	0.1	-0.6	0.3	0.
8	0		0.582	0.509	0.	0.	0.
9	0		1.59	1.59	0.	0.	0.
10	2	10	-0.5	0.	0.5	0.	25.
11	1		0.	0.	0.	0.	0.
12							
13	0	1	1.	1.	1.	1.	

Structure of the input deck for the example of Fig. 5-1.

CARD 1(A) FORMAT (18A4) Title card; use up to 72 columns.

This is a title card and is repeated in the output format. The letter (A) after CARD 1 refers to the format used as described above in Input data formats.

CARD 2(B) FORMAT (I2, I3, 4F10.5) MORE, IPOL, WAVE, ZSFAC, ZEFAC, ZMFAC

This is a control card; the same card is repeated at the end of the data set, but with MORE = 0 (last run for this data set) and IPOL = 1 (E-polarization).

MORE = 1 Another run will be made for this data set.

IPOL = 2 H-polarization.

WAVE = 1. Wavelength in units used. If geometry is normalized with respect to wavelength, WAVE = 1.

ZSFAC }  
ZEFAC } = 1. Relative multiplication factors for impedances.  
ZMFAC }

CARD 3(C) FORMAT (2I, 3X, 3F10.5) KODE, FIRST, LAST, INK

KODE = 1 Bistatic pattern is computed.

FIRST = 0. Initial incidence angle. Only for this incidence are the surface currents printed out.

LAST = 180. Final angle. Since the body is symmetrical about the y-plane, running as far as 360 degrees would be repetitious. The program requires that LAST > FIRST.

INK = 10. Scattering will be computed at 10-degree increments.

CARD 4(D) FORMAT (I2, I3, 5F10.5) TYPE, N, XA, YA, XB, YB, ANG

This and the next eight cards prescribe the scatterer geometry and associated electrical properties. The program requires that absorber surfaces be read in first. In this data set the following order of input is used: (1) frontal fin, (2) rear fins, (3) ogival cylinder.

TYPE = 1 Indicates this is an absorber surface.

N = 3 Number of sampling points on this segment.

XA = 0.5 }  
YA = 0 } Specifies endpoints for the segment.  
XB = 0.8 }  
YB = 0 }

ANG = 0. Implies that this is a straight line segment.

In generation of the geometry in subroutine GEOM it has been assumed that a body is symmetric about the  $y = 0$  axis, and only the parameters for the upper profile must be supplied. However, when a segment is a straight line and lies on the  $y = 0$  axis, its image is not generated. Such is the case here for CARD 4.

CARD 5(E) FORMAT (I2, 3X, 5F10.5) FORM, ZEA, ZEB, ZEX

This card prescribes the electrical sheet impedance parameters for the frontal strip.

FORM = 0 Selects equation for computation of ZE in ZFUN.

ZEA = (0.382, 0.509)  
ZEB = (0., 0.)  
ZEX = 0. } Electric impedance constants appropriate for the  
equation selected by FORM = 0. Note that in this  
particular case the value of ZEX is arbitrary.

CARD 6(F) FORMAT (I2, 3X, 5F10.5) FORM, ZMA, ZMB, ZMX

FORM = 0 Selects equation for computation of ZM in ZFUN

ZMA = (1.59, 1.59)  
ZMB = (0., 0.)  
ZMX = 0. } Magnetic impedance constants appropriate for the  
equation selected by FORM = 0.

CARD 7(D) FORMAT (I2, I3, 5F10.5) TYPE, N, XA, YA, XB, YB, ANG

This card specifies the geometry for the upper tail fin. Its format is the same as that of CARD 4. The lower fin (an image) will be generated automatically by the program.

CARD 8(E) FORMAT (I2, 3X, 5F10.5) FORM, ZEA, ZEB, ZEX

Since the same material is used in the tail fins as in the frontal fin, this card is identical to CARD 5.

CARD 9(F) FORMAT (I2, 3X, 5F10.5) FORM, ZMA, ZMB, ZMX

This card is identical to CARD 6.

CARD 10(D) FORMAT (I2,I3,5F10.5) TYPE, N,XA, YA, XY, YB, ANG

This card specifies the geometry for the upper portion of the ogival cylinder. Again, the lower portion will be generated automatically in the program.

TYPE = 2 Indicates this is an impedance surface.

XA = -0.5  
YA = 0.  
XB = 0.5  
YB = 0. } Specifies endpoints for the segment.

ANG = 25. Angle encompassed by the circular arc.

CARD 11(G) FORMAT (I2,3X,5F10.5) FORM, ZSA, ZSB, ZSX

This card specifies parameters for computation of normalized surface impedance ZS. Since the body is perfectly conducting, this card is easy to do, viz.

FORM = 1 Selects equation for computing ZS

ZSA = (0.,0.)  
ZSB = (0.,0.)  
ZEX = 0 } Surface impedance constants appropriate for the equation selected by FORM = 1.

CARD 12(H) FORMAT (I5)

Integer in column 5 shuts off reading of segment parameters.

CARD 13(I) FORMAT (I2,I3,4F10.5) MORE, IPOL, WAVE, ZSFAC, ZEFAC, ZMFAC

With the use of this card (in addition to MORE = 1 in CARD 2), computations for the same geometry are repeated, but for different electrical parameters. Here, only the polarization is changed (IPOL = 1), and since this is the last run for this data set, MORE = 0. Other entries are the same as in CARD 2.

MORE = 0 Last run for this data set.

IPOL = 1 E-polarization.

WAVE = 1. Wavelength.

ZSFAC }  
ZEFAC } = 1. Relative multiplication factor for impedances.  
ZMFAC }

### Output data:

The sample data set was run on the University of Michigan IBM 360/67 computer and the H-polarization results are shown in the following pages.

For the shape computed, there are a total of 29 sampling points on the body: 20 on the ogival cylinder and 9 on the absorber fins. The resultant matrix is 38 x 38 (MMK = 9+9+20), and 44.2 seconds of CPU time were required for both the E- and H-polarization computations.

The output consists of three major blocks and in this case each group requires a page of this report. On the first page (p. 41), geometrical and electrical input parameters are given, along with other useful data such as the radius and length of arcs used in generating the profile. Such output is helpful in verifying that all input parameters have been correctly punched and read into the machine.

The second block (p. 42) consists of geometrical and electrical parameters for all cells on the body, and includes the computed currents. When the incident wave direction is specified for a range of incident angles, the currents are printed out only for the first angle; if currents are required for other angles of incidence, the input data set must be repeated for the new incidence angle.

The third block (p. 43) lists an array of computed cross sections. Since there are three types of current contributing to the scattering, the individual contribution of each type is also given. These include electric current (ELECTRIC) and magnetic current (MAGNETIC) from the absorber sheets, and the surface current (IMPEDANCE) from the impedance surface. The (ABSORBER) column lists the net contributions of the absorber sheet (electric plus magnetic current), and the (TOTAL) column is the sum of the three contributions. Such a breakdown of the cross section into its components is often helpful in determining the sources of scattering (the dominant scatterer), analyzing the performance of the absorber, and studying other scattering effects.

The expressions used for computing the bistatic and backscattering cross sections are

OGIVAL-CYLINDR WITH FINS

SEG NUM	SEG NUM	-- ENDPOINTS OF SEGMENTS --				----- SEGMENT PARAMETERS -----								
NUM	TYP	CELLS	X A	Y A	X B	Y B	ANGLE	RADIUS	LENGTH	FORM	ZEA (ZMA)	ZFB (ZMB)	ZEX (ZMX)	
1	ABS	3	0.5000	0.0	0.8000	0.0	0.0	999.00	0.300	0	0.382	0.509	0.0	0.0
2	ABS	3	-0.4000	0.1000	-0.6000	0.3000	0.0	999.00	0.283	0	1.590	1.590	0.0	0.0
3	ABS	3	-0.4000	-0.1000	-0.6000	-0.3000	0.0	999.00	0.283	0	1.590	1.590	0.0	0.0
4	IMP	10	-0.5000	0.0	0.5000	0.0	25.00	2.31	1.008	1	1.590	1.590	0.0	0.0
5	IMP	10	-0.5000	-0.0	0.5000	-0.0	25.00	2.31	1.008	1	0.0	0.0	0.0	0.0

KEY PARAMETERS

INCIDENT POLARIZATION	H
SURFACE IMPEDANCE FACTOR	1.000
ELECTRIC IMPEDANCE FACTOR	1.000
MAGNETIC IMPEDANCE FACTOR	1.000
TOTAL NUMBER OF POINTS ON THE BODY	29
NUMBER OF SEGMENTS USED	5
NUMBER OF INCIDENT FIELD DIRECTIONS	19
NUMBER OF BISTATIC DIRECTIONS	0
WAVELENGTH	1.000



OGIVAL-CYLINDER WITH FINS

ABSORBER SURFACE

I	SEG	X	Y	S	DSQ	---	ZE	---	ZM	---	MOD (JE)	ARG (JE)	MOD (JM)	ARG (JM)
1	1	0.5500	0.0	0.0500	0.1000	0.382	0.509	1.590	1.590	0.0015	197.274	175.9988	130.740	
2	1	0.6500	0.0	0.1500	0.1000	0.382	0.509	1.590	1.590	0.0030	81.665	154.2007	95.055	
3	1	0.7500	0.0	0.2500	0.1000	0.382	0.509	1.590	1.590	0.0057	104.946	151.1338	46.245	
4	2	-0.4333	0.1333	0.0471	0.0943	0.382	0.509	1.590	1.590	0.6425	-56.877	127.6986	112.808	
5	2	-0.5000	0.2000	0.1414	0.0943	0.382	0.509	1.590	1.590	0.8052	-38.139	143.1452	141.711	
6	2	-0.5667	0.2667	0.2357	0.0943	0.382	0.509	1.590	1.590	0.7464	-26.004	154.7719	168.516	
7	3	-0.4333	-0.1333	0.0471	0.0943	0.382	0.509	1.590	1.590	0.6464	-59.428	128.3813	120.774	
8	3	-0.5000	-0.2000	0.1414	0.0943	0.382	0.509	1.590	1.590	0.8324	-38.695	132.1762	143.525	
9	3	-0.5667	-0.2667	0.2357	0.0943	0.382	0.509	1.590	1.590	0.7670	-24.537	142.6163	162.476	

IMPEDANCE SURFACE

I	SEG	X	Y	S	DSQ	---	ZS	---	MOD (JS)	ARG (JS)
10	4	-0.4507	0.0104	0.0504	0.1008	0.0	0.0	0.7305	174.281	
11	4	-0.3514	0.0279	0.1512	0.1008	0.0	0.0	0.8100	131.881	
12	4	-0.2515	0.0410	0.2520	0.1008	0.0	0.0	1.0088	81.928	
13	4	-0.1511	0.0498	0.3528	0.1008	0.0	0.0	1.2416	53.786	
14	4	-0.0504	0.0542	0.4536	0.1008	0.0	0.0	1.1703	28.453	
15	4	0.0504	0.0542	0.5544	0.1008	0.0	0.0	0.9292	-9.181	
16	4	0.1511	0.0498	0.6552	0.1008	0.0	0.0	0.9239	-61.240	
17	4	0.2515	0.0410	0.7560	0.1008	0.0	0.0	1.1662	-99.740	
18	4	0.3514	0.0279	0.8568	0.1008	0.0	0.0	1.2643	-125.755	
19	4	0.4507	0.0104	0.9576	0.1008	0.0	0.0	0.8253	-149.047	
20	5	-0.4507	-0.0104	0.0504	0.1008	0.0	0.0	0.7342	174.316	
21	5	-0.3514	-0.0279	0.1512	0.1008	0.0	0.0	0.8016	131.735	
22	5	-0.2515	-0.0410	0.2520	0.1008	0.0	0.0	1.0070	81.447	
23	5	-0.1511	-0.0498	0.3528	0.1008	0.0	0.0	1.2464	53.523	
24	5	-0.0504	-0.0542	0.4536	0.1008	0.0	0.0	1.1759	28.475	
25	5	0.0504	-0.0542	0.5544	0.1008	0.0	0.0	0.9294	-8.918	
26	5	0.1511	-0.0498	0.6552	0.1008	0.0	0.0	0.9192	-61.276	
27	5	0.2515	-0.0410	0.7560	0.1008	0.0	0.0	1.1644	-100.000	
28	5	0.3514	-0.0279	0.8568	0.1008	0.0	0.0	1.2661	-125.961	
29	5	0.4507	-0.0104	0.9576	0.1008	0.0	0.0	0.8240	-148.968	

BACKSCATTERING CROSS SECTION  
 $10 \cdot \log(\sigma/\lambda^2)$  (H-POLARIZATION)

THETA	(ELECTRIC)		(MAGNETIC)		(ABSORBER)		(IMPEDANCE)		(TOTAL)	
	DR	PHASE	DB	PHASE	DB	PHASE	DB	PHASE	DB	PHASE
0.0	-10.02	-38.07	-13.84	123.39	-17.16	-10.28	-21.36	102.80	-17.64	26.51
10.00	-10.69	-58.16	-13.87	111.68	-20.05	-37.09	-16.19	102.89	-19.87	63.86
20.00	-9.47	-109.19	-14.01	83.86	-16.55	-125.81	-9.32	99.91	-11.59	124.17
30.00	-7.11	-151.76	-16.71	49.02	-10.20	-161.40	-4.91	93.99	-4.82	125.39
40.00	-8.85	162.19	-19.20	-71.33	-10.21	178.79	-3.36	84.41	-2.55	108.80
50.00	-8.22	81.08	-9.56	-113.31	-19.52	132.56	-3.90	64.53	-3.29	72.77
60.00	-7.98	57.61	-9.98	-121.80	-21.72	55.32	-4.58	13.23	-3.70	18.05
70.00	-13.95	-168.20	-31.99	64.27	-14.60	-174.35	0.80	-26.66	-0.49	-32.71
80.00	-5.53	-137.74	-12.47	64.16	-9.87	-153.79	4.91	-35.30	4.25	-45.26
90.00	-20.51	-52.73	-29.24	173.19	-22.55	-72.15	6.36	-34.22	6.61	-35.44
100.00	-5.96	45.99	-10.10	-113.48	-12.46	18.35	5.17	-29.22	5.94	-24.13
110.00	-18.98	35.44	-14.13	-98.87	-16.90	-64.59	1.73	-18.00	1.52	-23.00
120.00	-5.61	-117.94	-18.73	52.35	-7.74	-115.22	-7.47	27.11	-11.39	-41.46
130.00	-7.07	-134.81	-16.32	69.72	-10.15	-146.59	-6.17	100.13	-6.55	137.48
140.00	-13.82	119.42	-25.09	-156.57	-12.94	133.14	-4.74	117.17	-1.96	121.63
150.00	-8.71	60.91	-14.10	-145.22	-13.61	85.51	-6.38	122.45	-4.05	110.92
160.00	-9.88	20.53	-13.13	-159.41	-20.02	20.39	-11.87	123.81	-11.99	101.10
170.00	-10.55	-22.98	-14.10	179.97	-17.17	-56.72	-18.30	120.11	-31.69	-42.78
180.00	-10.13	-39.60	-14.47	169.48	-15.25	-71.71	-23.70	112.67	-19.34	-74.36

$$\sigma/\lambda = \lim_{\rho \rightarrow \infty} \frac{2\pi}{\lambda} \rho \left| Y_0^S E_z^S \right|^2, \quad \text{E-polarization}$$

$$\sigma/\lambda = \lim_{\rho \rightarrow \infty} \frac{2\pi}{\lambda} \rho \left| H_z^S \right|^2, \quad \text{H-polarization}$$

and the associated phases are  $\text{Arg}(E^S)$  and  $\text{Arg}(H^S)$  for E- or H-polarization, respectively.

## VI CONCLUSIONS

In the previous sections a description of a computer program RAMVS for computation of scattering from a general two-dimensional body consisting of an arbitrary impedance cylinder and absorber sheets specified by equivalent electric and magnetic sheet impedances is given. The sheet impedances must be determined from the permittivity, permeability and thickness of the material, and then read in as input data. Consistent with the core limitations of the particular installation used to run the program, the program has the potential for solving scattering from many two-dimensional problems of interest. These include perfectly conducting bodies, bodies with prescribed surface impedance with or without absorber sheets present, and absorber-clad bodies. The RAM- series programs, such as RAMD (impedance body, E-polarization), REST (resistive sheets, E-polarization), or RASP (electric impedance sheets, E-polarization) developed and used under this contract are special cases of RAMVS. RAMVS was tested against these programs and, for the cases computed, gave the same results.

Many other aspects of RAMVS, however, have not been tested. To determine the capabilities as well as the shortcomings of the program, computed patterns should be compared against experimental measurements for structures such as isolated absorber sheets, sheets attached to metallic bodies, and thick absorber layers, either isolated or when coated on metallic cylinders. Of particular importance would be the determination of optimum cell size in absorber layers. Since there are two unknowns associated with each cell, it would be desirable to use cell sizes as large as possible, thereby minimizing the size of the matrix. On the other hand, cells that are too large may lead to a degradation of accuracy.

In retrospect, there are two areas in which the program could be modified. First, a substantial saving in computation time could be achieved by dispensing with the actual inversion of the matrix and solving the system of linear algebraic

equations by a direct technique such as Gaussian elimination (Southworth and Deleeuw, 1965). This would require developing, or obtaining if possible, an appropriate code to replace the subroutine FLIP. Additional changes might be required in MAIN and SMAIN to accommodate new variables, if such are needed. Before making such changes in the program, however, an accurate assessment of the CPU time should be made for a typical computation based on the matrix inversion approach and the direct solution technique. A "rule of thumb" is that it requires almost three times as many operations to invert a matrix as it does to solve the system of equations directly, but this applies only for a single incident vector. When a number of incident vectors are present, as is the case in computing backscattering patterns, it may be more efficient to invert the matrix and perform a simple multiplication with each incident vector, rather than to repeat a portion (back substitution) of a direct solution procedure for each.

The other possible modification of the program would be to add a capability to compute the tangential electric and magnetic fields along a prescribed surface and form the ratio of the two to determine the impedance. This would be helpful in relating the material properties of the coatings to surface impedances, especially near edges or other surface or electrical discontinuities, where no known analytical formulas exist. To change the present version to RAMVS to include this capability would require an additional subroutine for computing the electric and magnetic fields along a prescribed surface representing, for example, the outer surface of the absorber. Subroutines GEOM and SMAIN would have to be expanded to accommodate such a surface.

The next test for the program RAMVS will be to compute the scattering from the geometries the program was intended to handle. This will encompass scattering by ogival cylinders with magnetic fins ( $\epsilon_r = 1$ ), isolated absorber strips, and perhaps absorber-clad bodies. When possible, experimental data will be used for comparison. The results will be included in the Final Report under this contract.

APPENDIX  
PROGRAM LISTING

The following is an IBM version of the FORTRAN source listing of the program RAMVS. To run this program on a machine such as the CDC 6600 at WPAFB (AFAL), two cards should be changed in subroutine SMAIN as described in Section 5.1 of this report.



```

C-----C
C   F   FORMAT (I2,3X,5F10.5)  FORM,ZMA,ZMB,ZMX          C
C   FORM=-1      ZM(I)=(ZMA-ZMB*S(I))**ZMX              C
C   FORM= 0      ZM(I)=ZMA+ZMB*S(I)**ZMX                C
C   FORM= 1      ZM(I)=ZMA+ZMB*EXP(-ZMX*S(I))           C
C   ZMA,ZMB      COMPLEX IMPEDANCE CONSTANTS            C
C   ZMX          REAL IMPEDANCE CONSTANT                 C
C-----C
C           (DATA G AND H REQUIRED FOR EACH IMPEDANCE SEGMENT.) C
C   G   FORMAT (I2,I3,5F10.5)  TYPE,N,XA,YA,XB,YB,ANG    C
C   TYPE=1 ABSORBER SHEET                                     C
C   TYPE=2 IMPEDANCE SURFACE                                 C
C   N           NUMBER OF SAMPLING POINTS ON THIS SEGMENT C
C   XA,YA,XB,YB SEGMENT ENDPOINTS                           C
C   ANG        ANGLE SUBTENDED BY THE SEGMENT              C
C-----C
C   H   FORMAT (I2,3X,5F10.5)  FORM,ZSA,ZSB,ZSX          C
C   FORM=-1      ZS(I)=(ZSA-ZSB*S(I))**ZSX              C
C   FORM= 0      ZS(I)=ZSA+ZSB*S(I)**ZSX                C
C   FORM= 1      ZS(I)=ZSA+ZSB*EXP(-ZSX*S(I))           C
C   ZSA,ZSB      COMPLEX IMPEDANCE CONSTANTS            C
C   ZSX          REAL IMPEDANCE CONSTANT                 C
C-----C
C   I   FORMAT (I5)          INTEGER ZERO IN COLUMN 5 SHUTS OFF C
C                               READING OF SEGMENT PARAMETERS   C
C-----C
C           (USE THIS CARD ONLY IF, IN B, MORE=1)              C
C   J   FORMAT (I2,I3,4F10.5)  MORE,IPOD,WAVE,ZSFAC,ZEFAC,ZMFAC C
C
CCCCCCCCCCCCCCCCCCCCCCCCCCCCCCCCCCCCCCCCCCCCCCCCCCCCCCCCCCCC
C
C           *** DIMENSIONING FORMAT ***                        C
C-----C
C   VECTORS ARE DIMENSIONED ONLY IN THE MAIN PROGRAM.        C
C   IF K=NO. POINTS(CELLS) ON THE IMPEDANCE SURFACE AND      C
C   M=NO. OF POINTS(CELLS) ON THE ABSORBER SHEET, THEN      C
C           MK=M+K AND MMK=M+M+K                              C
C
C.....MAIN PROGRAM-----A STARTER PROGRAM                   C
C * COMPLEX A(MMK,MMK+1),PHI(MMK),PINK(MMK),LL(MMK),MM(MMK)  C
C * COMPLEX ZE(MK),ZM(MK)                                     C
C * DIMENSION X(MK),Y(MK),XN(MK),YN(MK),S(MK),DSQ(MK)       C
C * DIMENSION LUMP(2,MK)                                      C
C * DATA MI/MMK/                                            C
C   CALL SMAIN(MI,A,PHI,PINK,ZE,ZM,X,Y,XN,YN,S,DSQ,LL,MM,LUMP) C
C   END                                                       C
C           * CARDS TO BE CHANGED WHEN REDIMENSIONING        C
C
CCCCCCCCCCCCCCCCCCCCCCCCCCCCCCCCCCCCCCCCCCCCCCCCCCCCCCCCCCCC

```



C.....MAIN PROGRAM-----A STARTER PROGRAM

C\*\*\*\* RAMVS VERSION

COMPLEX A(150,151),PHI(150),PINK(150),LL(150),MM(150)

COMPLEX ZE(100),ZM(100)

DIMENSION X(100),Y(100),XN(100),YN(100),S(100),DSQ(100)

DIMENSION LUMP(2,100)

DATA MI/150/

CALL SMAIN(MI,A,PHI,PINK,ZE,ZM,X,Y,XN,YN,S,DSQ,LL,MM,LUMP)

END

```

SUBROUTINE SMAIN(MI,A,PHI,PINK,ZE,ZM,X,Y,XN,YN,
&S,DSQ,LL,MM,LUMP)
C**** RAMVS VERSION E-&H-POLARIZATIONS
DIMENSION LUMP(2,1)
COMPLEX A(MI,1)
COMPLEX PHI(1),PINK(1),ZE(1),ZM(1)
COMPLEX SUM,DEL,SUME,SUMM,SUMK
DIMENSION X(1),Y(1),XN(1),YN(1),S(1),DSQ(1),LL(1),MM(1)
DIMENSION ID(18),IPP(2)
COMMON/PIES/PI,TPI,PIT,PIPI,YZ,RED,DIG
REAL LAST,INK
DATA IPP/4HEEEF,4HHHHH/
C.....READ INPUT DATA AND GENERATE BODY PROFILE
5 READ(5,100,END=999) ID
READ(5,200) MORE,IPOL,WAVE,ZSFAC,ZEFAC,ZMFAC
READ(5,210) KODE,FIRST,LAST,INK
WRITE(6,150) ID
CALL GFORM(LUMP,X,Y,XN,YN,S,DSQ,ZE,ZM,K,M)
IF(KODE.NE.0) GO TO 25
NINC=1
NBIT=1+IFIX((LAST-FIRST)/INK)
GO TO 28
25 NBIT=0
NINC=1+IFIX((LAST-FIRST)/INK)
28 CONTINUE
C.....CONSTRUCT MATRIX ELEMENTS
M1=M+1
MK=M+K
MMK=MK+M
MM1=M1+M
DO 35 I=M1,MK
35 ZE(I)=ZE(I)*ZSFAC
FACE=ZEFAC*WAVE
FACM=ZMFAC*WAVE
XK=TPI/WAVE
DO 37 I=1,M
ZE(I)=ZE(I)*FACE
37 ZM(I)=ZM(I)*FACM
DO 39 I=1,MK
S(I)=S(I)/WAVE
39 DSQ(I)=DSQ(I)/WAVE
GO TO 50
40 FAC=ZSFAC/PZSFAC
DO 45 I=M1,MK
45 ZE(I)=ZE(I)*FAC
FAC=WAVE/PWAVE
FACE=ZEFAC/PZEFAC*FAC
FACM=ZMFAC/PZMFAC*FAC
DO 47 I=1,M
ZE(I)=ZE(I)*FACE
47 ZM(I)=ZM(I)*FACM
FAC=PWAVE/WAVE

```

```

XK=TPI/WAVE
DO 49 I=1,MK
S(I)=S(I)*FAC
49 DSQ(I)=DSQ(I)*FAC
50 CONTINUE
IF (IPOL.EQ.1) CALL MTXEL1(MI,M,K,X,Y,XN,YN,DSQ,ZE,ZM,A)
IF (IPOL.EQ.2) CALL MTXEL2(MI,M,K,X,Y,XN,YN,DSQ,ZE,ZM,A)
I=LUMP(2,MK)
WRITE(6,400) IPP(IPOL),ZSFAC,ZEFAC,ZMFAC,MK,I,NINC,NBIT,WAVE
C.....COMPUTE INCIDENT FIELD AND INVERT MATRIX
TETA=RED*FIRST
CT=COS(TETA)
ST=SIN(TETA)
DO 60 I=1,M
HOLD=-XK*(CT*X(I)+ST*Y(I))
DEL=CMPLX(COS(HOLD),SIN(HOLD))
PINK(I)=DEL
60 PINK(I+M)=-DEL*(XN(I)*CT+YN(I)*ST)
DO 63 I=M1,MK
HOLD=-XK*(CT*X(I)+ST*Y(I))
63 PINK(I+M)=CMPLX(COS(HOLD),SIN(HOLD))
CALL FLIP(A,MMK,MI,LL,MM,PINK,PHI,1)
WRITE(6,150) ID
C.....PRINT OUT STUFF FOR THE ABSORBER SURFACE (FIRST ANGLE ONLY)
WRITE(6,350)
WRITE(6,375)
DO 67 I=1,M
DEL=PHI(I)+(1.E-50,0.)
AMPE=CABS(DEL)
PHASEE=DIG*ATAN2(AIMAG(DEL),REAL(DEL))
DEL=PHI(I+M)+(1.F-50,0.)
AMPH=CABS(DEL)
PHASEH=DIG*ATAN2(AIMAG(DEL),REAL(DEL))
IF (IPOL.EQ.1) WRITE(6,395) (LUMP(J,I),J=1,2),X(I),Y(I),S(I),
&DSQ(I),ZE(I),ZM(I),AMPE,PHASEE,AMPH,PHASEH
67 IF (IPOL.EQ.2) WRITE(6,395) (LUMP(J,I),J=1,2),X(I),Y(I),S(I),
&DSQ(I),ZE(I),ZM(I),AMPH,PHASEH,AMPE,PHASEE
C.....PRINT OUT STUFF FOR THE IMPEDANCE SURFACE (FIRST ANGLE ONLY)
WRITE(6,300)
WRITE(6,325)
DO 65 I=M1,MK
IM=I+M
DEL=PHI(IM)+(1.E-50,0.)
AMP=CABS(DEL)
PHASE=DIG*ATAN2(AIMAG(DEL),REAL(DEL))
DEL=ZE(I)
65 WRITE(6,250) (LUMP(J,I),J=1,2),X(I),Y(I),S(I),DSQ(I),
&DEL,AMP,PHASE

```

```

C.....DOPE OUT THE APPROPRIATE FIELD FACTORS
WRITE (6,150) ID
THE=FIRST-INK
IF (KODE.EQ.1) GO TO 70
WRITE (6,800) FIRST,IPP(IPOL)
GO TO 75
70 WRITE (6,600) IPP(IPOL)
75 THE=THE+INK
IF (THE.GT.LAST) GO TO 105
IF (THE.EQ.FIRST) GO TO 85
TETA=RED*THE
CT=COS(TETA)
ST=SIN(TETA)
C.....IN THE FOLLOWING LOOP COMPUTE THE NEW INCIDENT FIELD
DO 80 I=1,M
HOLD=-XK*(CT*X(I)+ST*Y(I))
DEL=CMPLX(COS(HOLD),SIN(HOLD))
PINK(I)=DEL
80 PINK(I+M)=-DEL*(XN(I)*CT+YN(I)*ST)
DO 83 I=M1,MK
HOLD=-XK*(CT*X(I)+ST*Y(I))
83 PINK(I+M)=CMPLX(COS(HOLD),SIN(HOLD))
IF (KODE.EQ.0) GO TO 85
CALL FLIP(A,MMK,MI,LL,MM,PINK,PHI,2)
85 CONTINUE
C.....ADD UP THE CURRENTS FOR FAR FIELD
SUM=(1.E-25,0.)
SUME=SUM
SUMM=SUM
SUMK=SUM
DO 93 I=1,M
IM=I+M
DS=DSQ(I)
SUME=SUME-PHI(I)*PINK(I)*DS
93 SUMM=SUMM+PHI(IM)*PINK(IM)*DS
SUMM=SUMM*YZ
IF (IPOL.EQ.2) GO TO 90
DO 95 I=M1,MK
IM=I+M
95 SUMK=SUMK+(-1.+ZF(I)*(XN(I)*CT+YN(I)*ST))*PINK(IM)*DSQ(I)*PHI(IM)
GO TO 99
90 DEL=SUME
SUME=-SUMM/YZ
SUMM=DEL*YZ
DO 97 I=M1,MK
IM=I+M
97 SUMK=SUMK+(-ZF(I)+(XN(I)*CT+YN(I)*ST))*PINK(IM)*DSQ(I)*PHI(IM)
99 DEL=SUME+SUMM
SUM=DEL+SUMK
AMPR=REAL(SUME)
AMPI=AIMAG(SUME)
PHASEF=DIG*ATAN2(AMPI,AMPR)
AMPR=PI T*(AMPR*AMPR+AMPI*AMPI)

```

```

SCATE=10.*ALOG10(AMPR)
AMPR=REAL(SUMM)
AMPI=AIMAG(SUMM)
PHASEM=DIG*ATAN2(AMPI,AMPR)
AMPR=PIT*(AMPR*AMPR+AMPI*AMPI)
SCATM=10.*ALOG10(AMPR)
AMPR=REAL(DEL)
AMPI=AIMAG(DEL)
PHASED=DIG*ATAN2(AMPI,AMPR)
AMPR=PIT*(AMPR*AMPR+AMPI*AMPI)
SCATD=10.*ALOG10(AMPR)
AMPR=REAL(SUMK)
AMPI=AIMAG(SUMK)
PHASEK=DIG*ATAN2(AMPI,AMPR)
AMPR=PIT*(AMPR*AMPR+AMPI*AMPI)
SCATK=10.*ALOG10(AMPR)
AMPR=REAL(SUM)
AMPI=AIMAG(SUM)
PHASET=DIG*ATAN2(AMPI,AMPR)
AMPR=PIT*(AMPR*AMPR+AMPI*AMPI)
SCATT=10.*ALOG10(AMPR)
WRITE(6,900) THE, SCATE, PHASEE, SCATM, PHASEM, SCATD, PHASED,
&SCATK, PHASEK, SCATT, PHASET
GO TO 75
105 PZSFAC=ZSFAC
PWAVE=WAVE
PZFFAC=ZEFAC
PZMFAC=ZMFAC
IF (MORE.EQ.0) GO TO 5
READ (5,200) MORE, IPOL, WAVE, ZSFAC, ZEFAC, ZMFAC
WRITE (6,150) ID
GO TO 40
100 FORMAT (18A4)
150 FORMAT (1H1,18A4)
200 FORMAT (I2,I3,4F10.5)
210 FORMAT (I2,3X,3F10.5)
250 FORMAT(1H ,2I3,4F8.4,1X,2F11.3,F9.4,F9.3)
300 FORMAT(////18H0IMPEDANCE SURFACE)
350 FORMAT(17H0ABSORBER SURFACE)
325 FORMAT(8H0 I SEG,4X,1HX,7X,1HY,7X,1HS,6X,3HDSQ,
&11X,10H--- ZS ---,5X,7HMOD(JS),2X,7HARG(JS)/)
375 FORMAT(8H0 I SEG,4X,1HX,7X,1HY,7X,1HS,6X,3HDSQ,
&11X,10H--- ZE ---,13X,10H--- ZM ---,5X,7HMOD(JE),2X,7HARG(JE),2X,
&7HMOD(JM),2X,7HARG(JM)/)
395 FORMAT(1H ,2I3,4F8.4,2(1X,2F11.3),2(F9.4,F9.3))
400 FORMAT (////55X,14HKEY PARAMETERS//
&40X,21HINCIDENT POLARIZATION,22X,1A1//
&40X,24HSURFACE IMPEDANCE FACTOR,F20.3//
&40X,25HELECTRIC IMPEDANCE FACTOR,F19.3//
&40X,25HMAGNETIC IMPEDANCE FACTOR,F19.3//
&40X,34HTOTAL NUMBER OF POINTS ON THE BODY,I10//
&40X,23HNUMBER OF SEGMENTS USED,I21//

```

```

&40X,35HNUMBER OF INCIDENT FIELD DIRECTIONS,I9//
&40X,29HNUMBER OF BISTATIC DIRECTIONS,I15//
&40X,10HWAVELENGTH,F34.3)
600  FORMAT(///,51X,28HBACKSCATTERING CROSS SECTION,/,
&55X,20H10*LOG(SIGMA/LAMBDA),/,
&57X,1H(,1A1,14H-POLARIZATION),///,
&31X,10H(ELECTRIC),7X,10H(MAGNETIC),7X,10H(ABSORBER),7X,
&11H(IMPEDANCE),8X,7H(TOTAL),/,21X,5HTHETA,2X,
&5(17H  DB      PHASE  ))
800  FORMAT(///,49X,33HBISTATIC SCATTERING CROSS SECTION,/,
&55X,20H10*LOG(SIGMA/LAMBDA),/,
&48X,29HFOR INCIDENT FIELD DIRECTION=,F6.1,/,
&57X,1H(,1A1,14H-POLARIZATION),///,
&31X,10H(ELECTRIC),7X,10H(MAGNETIC),7X,10H(ABSORBER),7X,
&11H(IMPEDANCE),8X,7H(TOTAL),/,21X,5HTHETA,2X,
&5(17H  DB      PHASE  ))
900  FORMAT(19X,F7.2,5(1X,2F8.2))
999  RETURN
      END

```

```

SUBROUTINE GEOM(LUMP,X,Y,XN,YN,S,DSQ,ZE,ZM,K,M)
C**** RAMVS VERSION
COMPLEX ZEA,ZEB,ZMA,ZMB,ZFUN,ZE(1),ZM(1)
DIMENSION X(1),Y(1),XN(1),YN(1),DSQ(1),S(1)
DIMENSION LUMP(2,1)
COMMON/PIES/PI,TPI,PIT,PIPI,YZ,RED,DIG
I=0
K=0
L=0
M=0
WRITE (6,500)
C.....READ INPUT PARAMETERS AND PREPARE TO GENERATE SAMPLING POINTS
C.....IF TYPE=1 ABSORBER SHEET, M CELLS TOTAL
C.....IF TYPE=2 IMPEDANCE SURFACE, K CELLS TOTAL
C.....TYPE=1 SURFACE MUST BE READ IN FIRST
10 READ (5,200) ITYPE,N,XA,YA,XB,YB,ANG
IF (N.EQ.0) GO TO 120
LIM=2*N-1
READ (5,250) IZFRM,ZEA,ZEB,ZEX
IF (ITYPE.EQ.1) READ (5,250) IZMFRM,ZMA,ZMB,ZMX
TX=XB-XA
TY=YB-YA
D=SQRT(TX*TX+TY*TY)
IF (ANG.EQ.0.0) GO TO 20
T=0.5*RED*ANG
TRX=TX+TY/TAN(T)
TRY=TY-TX/TAN(T)
RAD=0.5*D/SIN(T)
ARC=2.0*RAD*T
ALF=T/N
DID=2.0*RAD*ALF
GO TO 30
20 RAD=999.
ARC=D
DID=D/N
C.....START GENERATING
30 LAST=2
IF(YA.EQ.0.0.AND.YB.EQ.0.0.AND.ANG.EQ.0.0) LAST=1
DO 110 JIM=1, LAST
L=L+1
DO 100 J=1,LIM,2
I=I+1
LUMP(2,I)=L
LUMP(1,I)=I
IF (I.EQ.1000) WRITE (6,400)
IF (JIM.EQ.2) GO TO 90
IF (ANG.EQ.0.0) GO TO 40
SINQ=SIN(J*ALF)
COSQ=COS(J*ALF)
X(I)=XA+0.5*(TRX*(1.0-COSQ)-TRY*SINQ)

```

```

      Y(I)=YA+0.5*(TRX*SINQ+TRY*(1.0-COSQ))
      XN(I)=-0.5*(TRX*COSQ+TRY*SINQ)/RAD
      YN(I)= 0.5*(TRX*SINQ-TRY*COSQ)/RAD
      GO TO 50
40    X(I)=XA+0.5*J*TX/N
      Y(I)=YA+0.5*J*TY/N
      XN(I)=-TY/D
      YN(I)= TX/D
50    ST=0.5*J*DID
      S(I)=ST
C.....COMPUTE THE ELECTRIC PARAMETERS
      IF(ITYPE.EQ.1) GO TO 60
C.....ZS IS STORED IN THE ZF VECTOR
      ZF(I)=ZFUN(IZEFRM,ZFA,ZEB,ZEX,ST)
      GO TO 100
60    ZM(I)=ZFUN(IZMFRM,ZMA,ZMB,ZMX,ST)
      ZE(I)=ZFUN(IZEFRM,ZEA,ZEB,ZEX,ST)
      GO TO 100
C.....FROM HERE TO 100 WE CREATE THE SEGMENT IMAGE
90    K=I-N
      X(I)=X(K)
      Y(I)=-Y(K)
      XN(I)=XN(K)
      YN(I)=-YN(K)
      S(I)=S(K)
      ZE(I)=ZE(K)
      ZM(I)=ZM(K)
100   DSO(I)=DID
      IF (JIM.EQ.1) GO TO 102
      YA=-YA
      YB=-YB
102   IF(ITYPE.EQ.1) GO TO 105
      WRITE(6,300) L,N,XA,YA,XB,YB,ANG,RAD,ARC,IZEFRM,ZEA,ZEB,ZEX
      K=I-M
      GO TO 110
105   WRITE(6,350) L,N,XA,YA,XB,YB,ANG,RAD,ARC,IZEFRM,ZEA,ZEB,ZEX
      WRITE(6,351) IZMFRM,ZMA,ZMB,ZMX
      M=J
110   CONTINUE
      GO TO 10
200   FORMAT (I2,I3,5F10.5)
250   FORMAT(I2,3X,5F10.5)
300   FORMAT(1H ,I2,5H  IMP,I4,1X,4F9.4,1X,2F7.2,F7.3,I4,1X,2F9.3,2X,
&2F9.3,F11.3)
350   FORMAT(1H ,I2,5H  ABS,I4,1X,4F9.4,1X,2F7.2,F7.3,I4,1X,2F9.3,2X,
&2F9.3,F11.3)
351   FORMAT(71X,I4,2H (,F8.3,1X,F8.3,3H) (,F8.3,1X,F8.3,3H) (,
&F8.3,1H))
400   FORMAT(37HWARNING: WE'VE GENERATED 1000 POINTS/)

```



```

500  FORMAT (13H0SEG SEG  NUM,3X,6H  -- ,21HENDPOINTS OF SEGMENTS,6H -
      &-- ,5X,27H ----- ,18HSEGMENT PARAMETERS,27H -
      &----- /          TYP CELLS,4X,2HXA,7X,2HYA,7X,
      &2HXB,7X,2HYB,6X,24HANGLE RADIUS LENGTH FORM,6X,8HZE(ZMA),12X,
      &8HZEB(ZMB),8X,8HZEX(ZMX)/)
120  RETURN
      END

```

```

      COMPLEX FUNCTION ZFUN(IFORM,ZA,ZB,ZEX,ST)
C**** RAMVS VERSION
      COMPLEX ZA,ZB
      IF(IFORM) 10,15,20
10   ZFUN=CEXP(ZEX*CLOG(ZA-ZB*ST))
      RETURN
15   ZFUN=ZA+ZB*ST**ZEX
      RETURN
20   ZFUN=ZA+ZB*EXP(-ZEX*ST)
      RETURN
      END

```

```

SUBROUTINE MTXFL1(MI,M,K,X,Y,XN,YN,DSQ,ZE,ZM,A)
C**** RAMVS VERSION E-POLARIZATION
DIMENSION X(1),Y(1),XN(1),YN(1),DSQ(1)
COMPLEX ZE(1),ZM(1),A(MI,1)
COMPLEX AA,HZ,HZA,HZB,H1,H1A,H1B
REAL NPDR,NDR,NDNP
COMMON/PIES/PI,TPI,PIT,PIPI,YZ,RED,DIG
MI=M+1
MK=M+K
DO 300 II=1,M
I=II
IM=II+M
XI=X(I)
YI=Y(I)
XNI=XN(I)
YNI=YN(I)
C.....GENERATE ELEMENTS IN 1,2,4, AND 5
DO 100 JJ=1,M
J=JJ
JM=J+M
DS=DSQ(J)
PDS=1./PIPI/DS
DDS=0.25*DS*DS
TPIDS=TPI*DS
TDS=TPIDS/24.
PITDS=PIT*DS
IF (I.EQ.J) GO TO 120
IJ=IABS(I-J)
IF (IJ.LE.2) GO TO 110
CALL DIST(XI,YI,X(J),Y(J),XNI,YNI,XN(J),YN(J),4,
&R,NPDR,NDR,NDNP,SDR,SPDR)
RK=R*TPI
CALL HANKC(RK,2,HZ,H1)
A(I,J)=HZ*PITDS
AA=H1*PITDS
A(I,JM)=YZ*CMPLX(0.,NPDR)*AA
A(IM,J)=CMPLX(0.,NDR)*AA
B=NPDR*NDR
AA=B*HZ+(SPDR*SDR-B)*H1/RK
A(IM,JM)= AA*PITDS*YZ
GO TO 100
110 CALL DIST(XI,YI,X(J),Y(J),XNI,YNI,XN(J),YN(J),5,
&R,NPDR,NDR,NDNP,SDR,SPDR)
B=R*R+DDS
C=DS*R*SPDR
RAK=TPI*SQRT(B+C)
IF (RAK.NE.RBK) GO TO 103
HZA=HZB
H1A=H1B
GO TO 105

```

```

103 CALL HANKC(RAK,2,HZA,H1A)
105 RBK=TPI*SQRT(B-C)
    RK=R*TPI
    CALL HANKC(RK,0,HZ,H1)
    CALL HANKC(RBK,2,HZB,H1B)
    AA=TDS*(HZA+4.*HZ+HZB)
    A(I,J)=AA
    A(IM,JM)=(0.25*SDR*(H1B-H1A)+NDNP*AA)*YZ
    AA=CMPLX(0.,-0.25)*SPDR*(HZB-HZA)
    A(I,JM)=AA*NPDR*YZ
    A(IM,J)=AA*NDR
    GO TO 100
120 AA=CMPLX(PIT,ALOG(DS)+0.02879837)*DS
    A(I,J)=ZE(J)+AA
    A(I,JM)=(0.,0.)
    A(IM,J)=(0.,0.)
    A(IM,JM)=(ZM(J)+CMPLX(0.,PDS)+AA)*YZ
100 CONTINUE
C.....GENERATE ELEMENTS IN 3 AND 6
    DO 300 JJ=M1,MK
        J=JJ
        JM=J+M
        PITDS=PIT*DSQ(J)
        CALL DIST(XI,YI,X(J),Y(J),XNI,YNI,XN(J),YN(J),4,
&R, NPDR, NDR, NDNP, SDR, SPDR)
        RK=R*TPI
        CALL HANKC(RK,2,HZ,H1)
C    ***REMEMBER ZS IS STORED IN ZE***
        HZA=ZE(J)
        AA=HZ-CMPLX(0.,NPDR)*H1*HZA
        A(I,JM)=AA*PITDS
        B=NPDR*NDR
        AA=B*HZ+(SPDR*SDR-B)*H1/RK
        AA=CMPLX(0.,NDR)*H1-AA*HZA
300 A(IM,JM)=AA*PITDS
        DO 500 II=M1,MK
            I=II
            IM=I+M
            XI=X(I)
            YI=Y(I)
            XNI=XN(I)
            YNI=YN(I)
C.....GENERATE ELEMENTS IN 7 AND 8
        DO 400 JJ=1,M
            J=JJ
            PITDS=PIT*DSQ(J)
            CALL DIST(XI,YI,X(J),Y(J),XNI,YNI,XN(J),YN(J),0,
&R, NPDR, NDR, NDNP, SDR, SPDR)
            RK=R*TPI
            CALL HANKC(RK,2,HZ,H1)
            A(IM,J)=HZ*PITDS
400 A(IM,J+M)=CMPLX(0.,NPDR)*H1*PITDS*YZ

```

```

C.....GENERATE ELEMENTS IN 9
  DO 500 JJ=M1,MK
    J=JJ
    IF (I.EQ.J) GO TO 510
    CALL DIST(XI,YI,X(J),Y(J),XNI,YNI,XN(J),YN(J),0,
&R, NPDR, NDR, NDNP, SDR, SPDR)
    RK=R*TPI
    CALL HANKC(RK,2,HZ,H1)
    AA=HZ-CMPLX(0.,NPDR)*H1*ZE(J)
    A(IM,J+M)=PIT*AA*DSQ(J)
    GO TO 500
510  DS=DSQ(J)
    A(IM,J+M)=0.5*ZE(J)+DS*CMPLX(PIT,ALOG(DS)+0.02879837)
500  CONTINUE
    RETURN
    END

```

```

SUBROUTINE MTXEL2(MI,M,K,X,Y,XN,YN,DSQ,ZE,ZM,A)
C**** RAMVS VERSION H-POLARIZATION
C**** RAMVS VERSION
DIMENSION X(1),Y(1),XN(1),YN(1),DSQ(1)
COMPLEX ZE(1),ZM(1),A(MI,1)
COMPLEX AA,HZ,HZA,HZB,H1,H1A,H1B
REAL NPDR,NDR,NDNP
COMMON/PIES/PI,TPI,PIT,PIPI,YZ,RED,DIG
M1=M+1
MK=M+K
DO 300 II=1,M
I=II
IM=II+M
XI=X(I)
YI=Y(I)
XNI=XN(I)
YNI=YN(I)
C.....GENERATE ELEMENTS IN 1,2,4, AND 5
DO 100 JJ=1,M
J=JJ
JM=J+M
DS=DSQ(J)
PDS=1./PIPI/DS
DDS=0.25*DS*DS
TPIDS=TPI*DS
TDS=TPIDS/24.
PITDS=PIT*DS
IF (I.EQ.J) GO TO 120
IJ=IABS(I-J)
IF (IJ.LE.2) GO TO 110
CALL DIST(XI,YI,X(J),Y(J),XNI,YNI,XN(J),YN(J),4,
&R,NPDR,NDR,NDNP,SDR,SPDR)
RK=R*TPI
CALL HANKC(RK,2,HZ,H1)
A(I,J)=HZ*PITDS*YZ
AA=H1*PITDS
A(I,JM)=CMPLX(0.,-NPDR)*AA
A(IM,J)=CMPLX(0.,NDR)*AA*YZ
B=NPDR*NDR
AA=B*HZ+(SPDR*SDR-B)*H1/RK
A(IM,JM)=-AA*PITDS
GO TO 100
110 CALL DIST(XI,YI,X(J),Y(J),XNI,YNI,XN(J),YN(J),5,
&R,NPDR,NDR,NDNP,SDR,SPDR)
B=R*R+DDS
C=DS*R*SPDR
RAK=TPI*SQRT(B+C)
IF (RAK.NE.RBK) GO TO 103
HZA=HZB
H1A=H1B
GO TO 105

```

```

103 CALL HANKC(RAK,2,HZA,H1A)
105 RBK=TPI*SQRT(R-C)
    RK=R*TPI
    CALL HANKC(RK,0,HZ,H1)
    CALL HANKC(RBK,2,HZB,H1B)
    AA=TDS*(HZA+4.*HZ+HZB)
    A(I,J)=AA*YZ
    A(IM,JM)=-0.25*SDR*(H1B-H1A)-NDNP*AA
    AA=CMPLX(0.,0.25)*SPDR*(HZB-HZA)
    A(I,JM)=AA*NPDR
    A(IM,J)=-AA*NDR*YZ
    GO TO 100
120 AA=CMPLX(PIT,ALOG(DS)+0.02879837)*DS
    A(I,J)=(ZM(J)+AA)*YZ
    A(I,JM)=(0.,0.)
    A(IM,J)=(0.,0.)
    A(IM,JM)=-ZE(J)-CMPLX(0.,PDS)-AA
100 CONTINUE
C.....GENERATE ELEMENTS IN 3 AND 6
    DO 300 JJ=M1,MK
        J=JJ
        JM=J+M
        PITDS=PIT*DSQ(J)
        CALL DIST(XI,YI,X(J),Y(J),XNI,YNI,XN(J),YN(J),4,
&R, NPDR, NDR, NDNP, SDR, SPDR)
        RK=R*TPI
        CALL HANKC(RK,2,HZ,H1)
C    ***REMEMBER ZS IS STORED IN ZE***
        HZA=ZE(J)
        AA=HZ*HZA-CMPLX(0.,NPDR)*H1
        A(I,JM)=AA*PITDS
        B=NPDR*NDR
        AA=B*HZ+(SPDR*SDR-B)*H1/RK
        AA=CMPLX(0.,NDR)*H1*HZA-AA
300 A(IM,JM)=AA*PITDS
        DO 500 II=M1,MK
            I=II
            IM=I+M
            XI=X(I)
            YI=Y(I)
            XNI=XN(I)
            YNI=YN(I)
C.....GENERATE ELEMENTS IN 7 AND 8
        DO 400 JJ=1,M
            J=JJ
            PITDS=PIT*DSQ(J)
            CALL DIST(XI,YI,X(J),Y(J),XNI,YNI,XN(J),YN(J),0,
&R, NPDR, NDR, NDNP, SDR, SPDR)
            RK=R*TPI
            CALL HANKC(RK,2,HZ,H1)
            A(IM,J)=HZ*PITDS*YZ
400 A(IM,J+M)=CMPLX(0.,NPDR)*H1*PITDS

```

```

C.....GENERATE ELEMENTS IN 9
  DO 500 JJ=M1,MK
  J=JJ
  IF (I.EQ.J) GO TO 510
  CALL DIST(XI,YI,X(J),Y(J),XNI,YNI,XN(J),YN(J),0,
&R, NPDR, NDR, NDNP, SDR, SPDR)
  RK=R*TPI
  CALL HANKC(RK,2,HZ,H1)
  AA=HZ*ZE(J)-CMPLX(0.,NPDR)*H1
  A(IM,J+M)=PIT*AA*DSQ(J)
  GO TO 500
510 DS=DSQ(J)
  A(IM,J+M)=0.5+DS*CMPLX(PIT,ALOG(DS)+0.02879837)*ZE(J)
500 CONTINUE
  RETURN
  END

```

```

SUBROUTINE DIST(XI,YI,XJ,YJ,XNI,YNI,XNJ,YNJ,I,
&R, NPDR, NDR, NDNP, SDR, SPDR)
C.....I=0 R, NPDR
C.....I=1 R, NPDR, NDR
C.....I=2 R, NPDR, NDR, NDNP
C.....I=3 R          NDNP, SDR, SPDR
C.....I=4 R, NPDR, NDR, SDR, SPDR
C.....I=5 R, NPDR, NDR, NDNP, SDR, SPDR
  REAL NPDR, NDR, NDNP
  IF (I.LT.0.OR.I.GT.5) GO TO 50
  RX=XI-XJ
  RY=YI-YJ
  R=SQRT(RX*RX+RY*RY)
  IF (I.EQ.3) GO TO 10
  NPDR=(RX*XNJ+RY*YNJ)/R
  IF (I.EQ.0) RETURN
  NDR=(RX*XNI+RY*YNI)/R
  IF (I.EQ.1) RETURN
  IF (I.EQ.4) GO TO 15
 10 NDNP=XNI*XNJ+YNI*YNJ
 15 IF (I.EQ.2) RETURN
  SDR=(RX*YNI-RY*XNI)/R
  SPDR=(RX*YNJ-RY*XNJ)/R
  RETURN
50 WRITE(6,90) I,R
90 FORMAT(31HOSICK DATA IN DIST *QUIT* I=,I2,2X,2HR=,E11.3)
  CALL SYSTEM
  END

```

```

SUBROUTINE HANKC(R,N,HZERO,HONE)
C.....HANKEL FUNCTIONS ARE OF FIRST KIND--J+IY
C..... N=0 RETURNS HZERO
C..... N=1 RETURNS HONE
C..... N=2 RETURNS HZERO AND HONE
C.....SUBROUTINE REQUIRES R>0
C.....SUBROUTINE ADAM MUST BE SUPPLIED BY USER
      DIMENSION A(7),B(7),C(7),D(7),E(7),F(7),G(7),H(7)
      COMPLEX HZERO,HONE
      DATA A,B,C,D,E,F,G,H/1.0,-2.2499997,1.2656208,-0.3163866,
&0.0444479,-0.0039444,0.00021,0.36746691,0.60559366,-0.74350384,
&0.25300117,-0.04261214,0.00427916,-0.00024846,0.5,-0.56249985,
&0.21093573,-0.03954289,0.00443319,-0.00031761,-0.00001109,
&-0.6366198,0.2212091,2.1682709,-1.3164827,0.3123951,-0.0400976,
&0.0027873,0.79788456,-0.00000077,-0.0055274,-0.00009512,
&0.00137237,-0.00072805,0.00014476,-0.78539816,-0.04166397,
&-0.00003954,0.00262573,-0.00054125,-0.00029333,0.00013558,
&0.79788456,0.00000156,0.01659667,0.00017105,-0.00249511,
&0.00113653,-0.00020033,-2.35619449,0.12499612,0.0000565,
&-0.00637879,0.00074348,0.00079824,-0.00029166/
      IF (R.LE.0.0) GO TO 50
      IF (N.LT.0.OR.N.GT.2) GO TO 50
      IF (R.GT.3.0) GO TO 20
      X=R*R/9.0
      IF (N.EQ.1) GO TO 10
      CALL ADAM(A,X,BJ)
      CALL ADAM(B,X,Y)
      BY=0.6366198*ALOG(0.5*R)*BJ+Y
      HZERO=CMPLX(BJ,BY)
      IF (N.EQ.0) RETURN
10  CALL ADAM(C,X,Y)
      BJ=R*Y
      CALL ADAM(D,X,Y)
      BY=0.6366198*ALOG(0.5*R)*BJ+Y/R
      HONE=CMPLX(BJ,BY)
      RETURN
20  X=3.0/R
      IF (N.EQ.1) GO TO 30
      CALL ADAM(E,X,Y)
      FOOL=Y/SQRT(R)
      CALL ADAM(F,X,Y)
      T=R+Y
      BJ=FOOL*COS(T)
      BY=FOOL*SIN(T)
      HZERO=CMPLX(BJ,BY)
      IF (N.EQ.0) RETURN

```



```
30 CALL ADAM(G,X,Y)
   FOOL=Y/SQRT(R)
   CALL ADAM(H,X,Y)
   T=R+Y
   BJ=FOOL*COS(T)
   BY=FOOL*SIN(T)
   HONE=CMPLX(BJ,BY)
   RETURN
50 WRITE(6,90) N,R
90  FORMAT(31HOSICK DATA IN HANKC *QUIT*  N=,I2,2X,2HR=,E11.3)
   CALL SYSTEM
   END
```

```
      SUBROUTINE ADAM(C,X,Y)
      DIMENSION C(7)
      Y=X*C(7)
      DO 10 I=1,5
10    Y=X*(C(7-I)+Y)
      Y=Y+C(1)
      RETURN
      END
```

```

SUBROUTINE FLIP(A,N,MI,L,M,X,Y,IAT)
COMPLEX A(MI,1),X(1),Y(1),D,BIGA,HOLD
DIMENSION L(1),M(1)
IF (IAT.GT.1) GO TO 150
D=CMPLX(1.0,0.0)
DO 80 K=1,N
L(K)=K
M(K)=K
BIGA=A(K,K)
DO 20 J=K,N
DO 20 I=K,N
10 IF (CABS(BIGA).GE.CABS(A(I,J))) GO TO 20
BIGA=A(I,J)
L(K)=I
M(K)=J
20 CONTINUE
J=L(K)
IF (J.LE.K) GO TO 35
DO 30 I=1,N
HOLD=-A(K,I)
A(K,I)=A(J,I)
30 A(J,I)=HOLD
35 I=M(K)
IF (I.LE.K) GO TO 45
DO 40 J=1,N
HOLD=-A(J,K)
A(J,K)=A(J,I)
40 A(J,I)=HOLD
45 IF (CABS(BIGA).NE.0.0) GO TO 50
D=CMPLX(0.0,0.0)
RETURN
50 DO 55 I=1,N
IF (I.EQ.K) GO TO 55
A(I,K)=-A(I,K)/BIGA
55 CONTINUE
DO 65 I=1,N
DO 65 J=1,N
IF (I.EQ.K.OR.J.EQ.K) GO TO 65
A(I,J)=A(I,K)*A(K,J)+A(I,J)
65 CONTINUE
DO 75 J=1,N
IF (J.EQ.K) GO TO 75
A(K,J)=A(K,J)/BIGA
75 CONTINUE
D=D*BIGA
80 A(K,K)=1.0/BIGA
K=N

```

```

100  K=K-1
      IF (K.LE.0) GO TO 150
      I=L(K)
      IF (I.LE.K) GO TO 120
      DO 110 J=1,N
      HOLD=A(J,K)
      A(J,K)=-A(J,I)
110  A(J,I)=HOLD
120  J=M(K)
      IF (J.LE.K) GO TO 100
      DO 130 I=1,N
      HOLD=A(K,I)
      A(K,I)=-A(J,I)
130  A(J,I)=HOLD
      GO TO 100
150  DO 200 I=1,N
      Y(I)=CMPLX(0.0,0.0)
      DO 200 J=1,N
200  Y(I)=A(I,J)*X(J)+Y(I)
      RETURN
      END

```

```

BLOCK DATA
COMMON/PIES/PI,TPI,PIT,PIPI,YZ,RED,DIG
DATA PI,TPI,PIT,PIPI,YZ,RED,DIG/3.1415927,6.2831853,
&1.5707963,9.8696044,0.0026525824,0.01745329,57.29578/
END

```

## REFERENCES

- Abramowitz, M. A. and I. A. Stegun (1964), Handbook of Mathematical Functions, NBS Appl. Math. Series No. 55, U. S. Government Printing Office, Washington, D. C. 20402, 369-370.
- International Business Machines (1966), IBM System/360 Scientific Subroutine Package (360A-CM-03X), Version II.
- Knott, E. F., V. V. Liepa and T. B. A. Senior (1973), "Non-Specular Radar Cross Section Study", The University of Michigan Radiation Laboratory Report No. 011062-1-F (AFAL-TR-73-70), Ann Arbor.
- Knott, E. F. and T. B. A. Senior (1974), "Non-Specular Radar Cross Section Study", The University of Michigan Radiation Laboratory Report No. 011764-1-T (AFAL-TR-73-422), Ann Arbor.
- Oshiro, F. K. (1973), "Computer Programs for Scattering from Two-Dimensional Bodies with Arbitrary Surface Impedance", Northrop Corporation, Aircraft Division Technical Report No. AFAL-TR-73-135.
- Southworth, R. W. and S. L. Deleeuw (1965), Digital Computations and Numerical Methods, McGraw-Hill Book Company, New York, 216-284.

## DOCUMENT CONTROL DATA - R &amp; D

(Security classification of title, body of abstract and indexing annotation must be entered when the overall report is classified)

1. ORIGINATING ACTIVITY (Corporate author) The University of Michigan Radiation Laboratory 2216 Space Research Bldg., North Campus Ann Arbor, Michigan 48105		2a. REPORT SECURITY CLASSIFICATION <b>UNCLASSIFIED</b>	
		2b. GROUP <b>NA</b>	
3. REPORT TITLE <b>SCATTERING FROM TWO-DIMENSIONAL BODIES WITH ABSORBER SHEETS</b>			
4. DESCRIPTIVE NOTES (Type of report and inclusive dates) <b>Technical                      Scientific                      Interim                      (15 October 1973 - 15 March 1974)</b>			
5. AUTHOR(S) (First name, middle initial, last name) <b>Valdis V. Liepa Eugene F. Knott Thomas B. A. Senior</b>			
6. REPORT DATE <b>March 1974</b>	7a. TOTAL NO. OF PAGES <b>69</b>	7b. NO. OF REFS <b>6</b>	
8a. CONTRACT OR GRANT NO. <b>F33615-73-C-1174</b>	9a. ORIGINATOR'S REPORT NUMBER(S) <b>011764-2-T</b>		
b. PROJECT NO. <b>7633</b>	9b. OTHER REPORT NO(S) (Any other numbers that may be assigned this report) <b>AFAL-TR-74-119</b>		
c. Task No. <b>7633-13</b>			
d.			
10. DISTRIBUTION STATEMENT <b>Distribution limited to U. S. Government Agencies only; Test and Evaluation Data; May 1974 Other requests for this document must be referred to AFAL/WRP</b>			
11. SUPPLEMENTARY NOTES		12. SPONSORING MILITARY ACTIVITY <b>Air Force Avionics Laboratory Air Force Systems Command Wright-Patterson Air Force Base, Ohio</b>	
13. ABSTRACT <p>This report describes a program that computes the far field scattering pattern of a two-dimensional cylindrical body (or bodies) treated with absorbing materials. The body surface is assumed to satisfy an impedance boundary condition and the absorber is modeled by equivalent electric and magnetic sheets. The program reduces the coupled integral equations governing the surface currents to a system of simultaneous linear equations, solves for the unknown currents, and then computes the far field pattern from the solution. The integral equations derived and presented in a previous interim report were used as the basis for preliminary versions of the program, but these equations have been found to be in error. The required correction consists of incorporating terms previously omitted and the corrected equations are presented and discussed. Careful attention is given to a description of the input data necessary to run the program and the results of a sample run are included for illustration.</p> <p>The program was developed to explore the effects of absorbent materials on the scattering of electromagnetic waves by edges. Programs used previously in similar explorations embodied a surface impedance boundary condition; for lossy materials covering smooth surfaces of large radius of curvature, such an impedance can be estimated from the layer thickness and material properties, but the relationship breaks down near edges. The program described in this report, however, models the effects of actual materials rather than using the nebulous surface impedance boundary condition.</p>			

14. KEY WORDS	LINK A		LINK B		LINK C	
	ROLE	WT	ROLE	WT	ROLE	WT
far field scattering cylindrical body two-dimensional absorber sheets surface currents computer program integral equations impedance surfaces radar cross section radar camouflage radar absorber material						